Salatiel Gonçalves Neto

Como a delimitação de zonas adaptativas a partir de filogenia ou ecologia afeta a inferência de extinção dependente da idade?

Do phylogenetically and ecologically delimited adaptive zones affect our inference of age-dependent extinction?

São Paulo

2023

Salatiel Gonçalves Neto

Como a delimitação de zonas adaptativas a partir de filogenia ou ecologia afeta a inferência de extinção dependente da idade?

Do phylogenetically and ecologically delimited adaptive zones affect our inference of age-dependent extinction?

Versão corrigida

Dissertação apresentada ao Instituto de Biociências da Universidade de São Paulo, para a obtenção de Título de Mestre em Mestre em Ciências, na Área de Ecologia de Ecossistemas Terrestres e Aquáticos.

Orientador: Tiago Bosisio Quental

São Paulo

2023

Ficha Catalográfica

Gonçalves-Neto, Salatiel

Como a delimitação de zonas adaptativas a partir de filogenia ou ecologia afeta a inferência de extinção dependente da idade?

76 p.

Dissertação (Mestrado) - Instituto de Biociências da Universidade de São Paulo. Departamento de Ecologia.

1. Macroevolução 2. Extinção independente de idade 3. Hipótese da Rainha Vermelha

I. Universidade de São Paulo. Instituto de Biociências. Departamento de Ecologia.

Comissão Julgadora:

Prof.(a). Dr(a).

Prof.(a). Dr(a).

Prof.(a). Dr(a).

Prof. Dr. Tiago Bosisio Quental

Orientador

Agradecimentos

Esta dissertação não teria sido concluída com sucesso sem a ajuda e apoio essenciais de diversas pessoas ao longo desta jornada. Gostaria de começar expressando minha profunda gratidão ao meu orientador, Tiago Quental, por sua orientação, paciência e incentivo ao longo deste processo. Além disso, agradeço sinceramente aos membros do comitê de acompanhamento, Lee Hsiang Liow e Graham Slater, pelas valiosas contribuições que enriqueceram este estudo. Agradeço, também os membros do LabMeMe pelo ambiente estimulante que contribuiu significativamente para o meu desenvolvimento como cientista e para a conclusão deste trabalho. Também expresso minha gratidão a todos os professores que contribuíram ao longo do meu período de mestrado.

A minha família merece um agradecimento especial por seu constante encorajamento e amor. Desde cedo, eles me incentivaram nos estudos, e suas palavras de estímulo foram um verdadeiro suporte durante toda a minha formação acadêmica. Aos meus amigos da graduação na UNICAMP, agradeço por compartilharem, mesmo à distância, essa jornada acadêmica comigo e por proporcionarem momentos valiosos de descontração e conversas sobre a vida.

Quero expressar minha sincera gratidão a Vera pela assistência nas questões burocráticas e pelo apoio na resolução de dúvidas que surgiram ao longo deste caminho. Por último, gostaria de agradecer ao departamento de Ecologia e à FAPESP pelo suporte financeiro que tornou este projeto possível. Este trabalho foi realizado com o financiamento da Fundação de Amparo à Pesquisa do Estado de São Paulo (FAPESP), processo nº 2021/04258-9.

A todos vocês, minha sincera gratidão por terem feito parte desta jornada e por terem contribuído de maneira tão significativa para o sucesso desta dissertação e para a minha formação acadêmica.

Table of Contents

INTRODUCTION

Biological diversity displays an uneven distribution across various regions, evolutionary lineages, and even spans of time. Prominent instances of this disparity include the latitudinal species gradient (Hillebrand, 2004; Mittelbach *et al.*, 2007); the striking disparity between the living Squamata group (comprising over 10,000 species) and its sister lineage, the living tuataras with just one species (Stanley, 1979); and the dramatic drop in species numbers after a mass extinction event (Raup & Sepkoski, 1982; Bambach, 2006). In order to comprehend the disparity in species diversity, it is essential to examine the underlying dynamics of diversification and its variations across regions, lineages, and time periods. When considering a global or clade perspective, the quantity of species hinges on the equilibrium between the rate of speciation (the pace at which new species emerge) and the rate of extinction (the pace of species disappearance). While this basic view offers an initial framework for explaining fluctuations in species richness, a comprehensive understanding of these imbalances necessitates an exploration of the factors that drive changes in speciation and extinction rates (Ezard *et al.*, 2016).

The comprehension of biodiversity regulators has sparked divergent opinions on abiotic versus biotic controls (Jablonski, 2008; Benton, 2009). At deep time, biotic controls are often discussed in terms of evolutionary shifts in body size, adaptability, and ecological interactions, particularly competition (Benton, 2009). On the contrary, abiotic controls encompass alterations in the physical environment and fluctuations in climate (Benton, 2009). In the context of deep-time analysis, the most profound shifts in biodiversity have traditionally been attributed to abiotic factors (Benton, 2009; Condamine *et al.*, 2013), relegating biotic interactions to a secondary role (Benton, 2009). This dichotomy is also referred to as the Red Queen and Court Jester hypothesis (Barnosky, 2001; Benton, 2009). Within this framework, Benton (2009) posits that the influence of these factors could be linked to different temporal scales, with biotic factors (Red Queen) holding greater relevance in shorter time spans, while abiotic factors (Court Jester) play a more pivotal role in deep-time contexts. Recent studies propose that biotic interactions might hold more significance than previously assumed (Silvestro *et al.*, 2015; Liow *et al.*, 2015; Pires *et al.*, 2017; Jouault *et al.*, 2022) and that their previous secondary role could be more due to our initial incapacity to adequately test such factors. While the dichotomous perspective has undeniably facilitated the exploration of the effects of biotic and abiotic factors, it has become evident that we must study their interplay to gain a deeper understanding of biodiversity regulators (Ezard *et al*., 2011; Condamine *et al*., 2020).

Although Van Valen (1973) did not solely propose biotic factors as the exclusive focus of his Red Queen hypothesis, the appreciation for biotic controls on biodiversity has certainly grown following his work. Building on linear survivorship curves (presented on a semi-logarithmic scale), Van Valen (1973) asserted that extinction occurs at a consistently stochastic rate within an adaptive zone or an ecologically homogeneous group, resulting in an equal chance of species going extinct at any given point in time, suggesting that the probability of extinction was unrelated to the age of a lineage. This pattern is termed "The Law of Constant Extinction" (Van Valen, 1973). While the slope of this linear relationship may vary (and consequently the average extinction rate) among larger taxonomic groups, Van Valen (1973) indicated that this linear relationship seems to be nearly ubiquitous across all forms of biodiversity when looking at individual clades. He introduced the Red Queen hypothesis as a mechanism to account for his "law" (Van Valen, 1973), relying on the concept of adaptive zones coined by G.G. Simpson some years earlier (Simpson, 1944).

According to Simpson (1944), adaptive zones describe a collection of physical and biotic situations utilized by different species that share common traits and patterns of habitat use. An adaptive zone could be characterized as: "*the sum of the physical and biotic situations that an organism or a group of ecologically and/or evolutionarily related entities lives and evolves in. This can be thought of as the niche of a higher tax on. It is itself evolvable and particular adaptive zones might be unfilled by organisms at a given time*" (Liow *et al*., 2011). Understanding adaptive zones revolves around the utilization of resources such as food and space (Van Valen, 1971). Hence, in accordance with Van Valen's Red Queen hypothesis, within a given adaptive zone, lineages must perpetually adapt to match the ever-changing environment. It's within this adaptive zone that the "Law of Constant Extinction" becomes apparent. At the core of Van Valen's argument is the notion that the total amount of resources (or energy) remains constant, framing evolution as a zero-sum game. In this paradigm, any evolutionary advantage gained by one lineage is offset by an equivalent disadvantage for a potential competitor (or predator) within the same adaptive zone. Therefore, evolution as proposed by Van Valen is a memoryless process and age should not influence a given lineage's probability of extinction. Van Valen's original Red Queen hypothesis formulation (Van Valen, 1973), underscores the pivotal role of the adaptive zone in his framework (see also a review by Liow *et al*., 2011). Within an adaptive zone, —whether closely related or not—engage in competition for energy, (note that predator-prey relationships also belong in this dynamics). The dynamics of a zero-sum game predominantly unfold within the adaptive zone, wherein the evolutionary advancement of one taxon corresponds to a negative impact of equal magnitude on another taxon (Van Valen, 1973; also discussed in Stenseth & Smith, 1984). This framework aligns with the idea that resource constraints within the adaptive zone contribute to the memoryless nature of evolutionary processes, reinforcing the age-independency of extinction probabilities.

After Van Valen's seminal work, very few studies have been conducted on this specific topic. Nevertheless, the vast majority of studies that have examined clades at the species level have demonstrated age-dependent extinction (Januario & Quental, 2021, and references therein). These examples generally present either positive age dependency —an increase in the probability of extinction linked to age (Pearson, 1995; Parker & Arnold, 1997; Doran *et al.*, 2006; Ezard *et al.*, 2011) or negative age dependency —a decrease in the probability of extinction linked to age (Jones & Nicol 1986; Finnegan *et al.*, 2008; Crampton *et al.*, 2016; Hagen *et al.*, 2018; Silvestro *et al.*, 2020). The rationales behind negative age-dependent extinctions generally draw upon stochastic demographic effects associated with population size and geographical range. Under this premise, newly formed species usually commence with smaller populations and limited ranges, consequently facing an increased probability of extinction (Rosenblum *et al*., 2012). Over time, as species age, they tend to experience an increase in both their population size and the extent of their distribution area (Miller, 1997; Liow & Stenseth, 2007). This expansion ultimately leads to a decrease in their susceptibility to extinction (Payne & Finnegan, 2007; Foote *et al*., 2008; Jablonski, 2008).

A biological explanation for positive age dependency could entail what is known as an evolutionary ratchet mechanism that causes "species senescence" and reduced evolvability, which increases the probability of extinction with advancing age (akin to the process discussed by Muller, 1964). Because back mutations are extremely rare, Muller's ratchet (Muller, 1964) suggests that populations of clonal organisms will progressively accumulate harmful mutations through drift. As a result, over time, a growing number of inferior genotypes dominate the population, and these are less likely to endure when environmental disturbances occur. Similarly, the macroevolutionary ratchet could operates through the evolution of specialization, such as increased in body mass and specialized dentition in carnivore (Van Valkenburg, 1999). This occurs as the process of speciation tends to generate increasingly specialized forms. Considering the infrequency of evolutionary reversals, clades that present a tendency for evolutionary transition between young, generalist, extinction resistant population toward old, specialized population are theorized to face disadvantage as the biotic and abiotic condition changes (Pearson, 1995; Van Valkenburg, 1999; Doran *et al*., 2006). Alternatively, the positive age-dependency could be explained under a scenario of morpho-ecological stasis, where old species may not be able to compete against new species (Pearson, 1995; Eldredge *et al.,* 2005).

The discrepancy observed between Van Valen's original work and subsequent studies can be understood by considering the different taxonomic levels employed in these investigations (Januário & Quental, 2021). In his initial research, Van Valen assumed that higher taxonomic categories could serve as proxies for understanding dynamics at the species level. However, among the 25,000 sub-taxa distributed across 46 distinct clades, only four clades were studied at the species level. Although these few cases exhibited age-independent extinction, the majority of subsequent studies conducted at the species level demonstrated age-dependent extinction (Januário & Quental, 2021). It's worth noting that only a limited number of researchers have explored the implications of using various taxonomic levels when inferring age-dependent extinction patterns. Pearson (1995) found positive age dependency in both species and genera of trilobites. In a preliminary study, Ezard *et al*. (2016) investigated planktonic macroperforate foraminifera and uncovered distinct patterns depending on the taxonomic level employed — species versus genus. Specifically, the species level displayed positive age dependency, while age dependency was notably absent at the genus level. In more recent work, Januario & Quental (2021) examined fossils of ruminants and identified negative age dependency at the species level, contrasting with age independence at the genus level.

The majority of studies aimed at investigating age-dependent extinction have typically examined this empirical pattern by categorizing their study groups through phylogenetic or taxonomic criteria (e.g., Pearson, 1995; Crampton *et al.*, 2016; Condamine *et al.*, 2019; Silvestro *et al.*, 2020). These studies have generally not explicitly integrated ecological considerations, except for assuming that species within each clade share ecological similarities (which may be a reasonable assumption for many groups). However, a noteworthy exception exists in the work of Ezard *et al*. (2011) concerning planktonic foraminifera. Their research revealed evidence supporting positive age-dependent extinction when explicitly factoring in ecology (alongside other variables such as climate). The difficulty of identifying the pool of species belonging to a given adaptive zone is echoed in Van Valen's work (1973), where the challenge of defining these homogeneous groups is briefly discussed, but higher taxa were used as a convenient approximation for such adaptive zones. However, when delving into the interpretation of the "Law of Constant Extinction" and exploring the Red Queen hypotheses, it becomes evident that Van Valen fundamentally viewed adaptive zones through the lens of an ecologically defined pool of species. Simpson (1944, 1953), early on recognized that the convergent evolution often leads to related species belonging to a given adaptive zone. Consequently, for practical convenience, it has become common to predominantly characterize adaptive zones based on taxonomic criteria. However, Simpson (1953) underscored that the concept was not tied to taxonomy. Although subsequent work continued to use a taxonomically or phylogenetically defined pool of species when testing the "Law of Constant Extinction" (e.g., Pearson, 1995; Crampton *et al*., 2016; Condamine *et al*., 2019; Silvestro *et al*., 2020), an ecologically defined pool of species would more closely align with Van Valen's original idea of the adaptive zone and his underlying Red Queen hypothesis. Defining the species pool through the grouping of species based on ecological traits, rather than solely relying on phylogenetic identity, would align more closely with Van Valen's original view of the adaptive zone. This approach might better reflect a scenario where species engage in more intricate "interactions" with one another, thereby wielding a more pronounced influence on their evolutionary trajectories and probability of extinction. Additionally, differences in ecology (or morphological traits used as a proxy for ecology) have been shown to affect extinction probabilities (Van Valkenburgh 1999; Chichorro *et al*., 2019; Hembry & Weber, 2020; Zeng & Wiens 2021), implying that considering such effects when attempting to examine age-dependent extinction probability could be an important step toward gaining a deeper understanding of extinction risk.

We used the North American Canidae fossil record to investigate how different pools of species (i.e. phylogenetic pool and ecological pool) affect our capacity to understand the "Law of Constant Extinction". The distinct phylogenetic pools of species were based on well-defined taxonomy. Specifically, we delineated the entire Canidae family and its three subfamilies—Hesperocyoninae, Borophaginae, and Caninae as different phylogenetic defined pool of species. This delimitation of the species pool followed the same criteria used in previous studies. The ecological pools of species were defined according to distinct ecological guilds found in the Canidae family — specifically, hypercarnivores, mesocarnivores, and hypocarnivores. This approach allowed us to examine the effect of age on extinction under an explicit ecologically defined adaptive zone. Using morphological characters and what we know from extant species, extinct species can be (and in fact have been) characterized into hypocarnivores (small predators that use invertebrates and plant material and consume less than 30% of vertebrate material), mesocarnivores (a diet of about 50 to 70% of vertebrate material), and hypercarnivores (more than 70% of its diet consists of large-vertebrates preys) (Van Valkenburgh, 1991; Wang & Tedford, 2008; Slater, 2015). This dietary classification allowed us to construct a species pool explicitly defined by ecological traits to investigate the potential effect of age on the probability of extinction. Defining species based on guilds not only offers a representation of an adaptive zone more similar to Van Valen's original work but also takes into account the fact that these ecological guilds have demonstrated significant macroevolutionary consequences. For instance, hypercarnivores and hypocarnivores exhibit abbreviated lineage durations (Van Valkenburgh & Damuth, 2004; Balisi *et al*., 2018). The Canidae family has a well-documented fossil record both in space and time (Wang, 1994; Wang *et al.*, 1999; Tedford *et al.*, 2009). Additionally, there are thorough ecomorphological characterizations available for the majority of both extinct and extant species (Janis *et al*., 1998; Van Valkenburgh *et al*., 2004; Slater, 2015; Balisi *et al*., 2018; Balisi & Van Valkenburgh, 2020). Lastly, this family's evolutionary history is largely centered in North America (Wang & Tedford, 2008), having a well-defined geographical arena, and reveals a diverse spectrum of body sizes and dietary preferences.

More specifically we tested the following hypothesis: 1- The signal of age-independency is more evident in the ecological pool of species than in a phylogenetic pool of species. If the pool choice interferes with our inference of age-dependency extinction, the different pools of species (phylogenetic and ecological) are expected to show different signals of age-dependency extinction. If the ecological pool of species genuinely provides a more accurate representation of the adaptive zone used by Van Valen (1973), and if his Red Queen mechanism indeed stands as the primary force steering age-independent extinction, we hypothesize a heightened visibility of the age-independent signal within the ecological pool of species; In the case that the first hypothesis is rejected, the different ecologies might predispose species to age differently with respect to their chance of extinction, and hence show different signals of age-dependency. 2- When compared to other dietary guilds, hypercarnivores would show a stronger signal of negative age-dependent extinction. This expectation was based on previous work that showed that: 1- smaller species have greater population density relative to those of larger species (Damuth, 1981; Damuth, 1987); 2- higher population density is presumed to lower the probability of extinction (Purvis *et al*, 2000); 3- the level of carnivory is related to body size (Valkenburgh *et al.*, 2004; but see Balisi & Van Valkenburg, 2020); 4- large body size is related to small litter and slow reproduction rates which could enhanced extinction probability (McKinney, 1997; Purvis *et al.*, 2000). We note however that large hypercarnivores also have large geographical distributions which typically decrease the probability of extinction (Payne & Finnegan, 2007; Foote *et al*., 2008; Jablonski, 2008). Given the relationship between body size/diet and population demographic aspects, we expect that hypocarnivores, and to a lesser extent mesocarnivores, should typically start with a larger population size and with higher population growth than hypercarnivores, and hence, be less prone to demographic effects than hypercarnivores, typically evoked as underlying processes of a negative age-dependent extinction.

METHODS

Ecomorphological data

We downloaded and curated data on body mass and craniodental variables from two different sources. We downloaded body mass information and measurements of the lower first molar (m1) for our 133 canid species from the dataset published by Faurby *et al.* (2021), which compiles information from various literature sources. Craniodental measurements, including relative blade length of the lower first molar (RBL), lower first molar blade size relative to dentary (lower jaw) length (M1BS), the size of the lower second molar relative to the dentary (lower jaw) length (M2S), the mechanical advantage of the temporalis muscle (MAT), the robustness of the lower fourth premolar (p4S), and relative lower molar grinding area (RLGA) were taken from the dataset published by Slater (2015). These craniodental variables were used to characterize the diet of all fossil species (see analysis details below). Following the approach described by Slater (2015) who successfully classified 91 fossil canids into three dietary categories (hypercarnivores, mesocarnivores, and hypocarnivores), we used the same set of variables plus RLGA. These variables have been suggested as reliable indicators of dietary groups in canids (Van Valkenburg & Koepfili, 1993).

Due to the nature of fossil material, our dataset exhibited varying degrees of missing data, ranging from 28% to 48%, with an average of 35%. Among the variables, p4S had the lowest percentage of missing data, while MAT had the highest. However, we had complete information on m1 measurements for all species. To address the issue of missing data, we applied a phylogenetically informed imputation approach, which allowed us to estimate values for the missing data points based on the available information.

Data imputation

There are various approaches employed to deal with missing data. A commonly used approach is the “complete-case analysis”, where observations with missing values are excluded. However, this approach can lead to a loss of information and potentially introduce bias into the results (Johnson *et al.*, 2020; Debastiani *et al.*, 2021). An alternative approach is data imputation, which has been recommended and considered a better approach for handling missing data over “complete-case analysis” (Penone *et al*., 2014; Kim *et al*., 2018; Johnson *et al.*, 2020). Additionally, incorporating phylogenetic information has been demonstrated to improve the estimation of missing data (Penone *et al.*, 2014; Molina-Venegas *et al.*, 2018; Johnson *et al.*, 2020). The use of phylogenetic information in the imputation process is based on the understanding that species closely related tend to be more similar, on average, than distantly related ones - a phenomenon known as phylogenetic signal (Pagel, 1999; Blomberg *et al*., 2003).

Here, we used a phylogenetically informed imputation approach implemented in the R package *Rphylopars* (Goolsby *et al*., 2017) to impute the missing ecomorphological data. This method uses a phylogeny to estimate the across-species and within-species trait covariance to impute missing values (Goolsby *et al*., 2017). It is worth considering that this method works better when there is a strong phylogenetic signal in the traits. If a trait has a low signal the phylogeny may introduce noise and the imputed values could exhibit a high variance (Goolsby *et al.*, 2016; Johnson *et al.*, 2020). To assess the phylogenetic signal of our traits, we utilized the *phylosig* function from the R package *phytools* (Revell, 2012) to calculate Pagel's lambda (λ) for all craniodental variables. Our estimation revealed a high phylogenetic signal ($\lambda > 0.8$) in 6 out of the 7 tested craniodental variables (Fig. S1). We imputed the values for those 6 traits with strong phylogenetic signals using a Lambda model for trait evolution. We used 1000 Carnivora trees provided by Faurby *et al*. (2019) for the estimation of phylogenetic signal and in the imputation process. The trees were pruned to keep only canid species using the function *keep.tip* from the R package *ape* (Paradis *et al.,* 2004). The final ecomorphological dataset included observed and imputed values for the 6 craniodental variables for 133 canid species, as well as observed values for the MAT variable for 68 extant and fossil species. While we did not impute the MAT variable due to its low phylogenetic signal, it was utilized in the ecological characterization of 61 fossil species.

Ecological categorization using discriminant analysis.

Following Slater (2015), we used a Linear Discriminant Analysis (LDA) to characterize the diet of fossil species. LDA is a statistical method used for both dimensionality reduction and classification. The goal of this approach is to find a linear transformation that maximizes class discrimination by maximizing the separation between classes while minimizing the variability within each class (Venables & Ripley, 2002). We used an LDA implemented in the *Applied Statistics with S* (MASS) (Venables & Ripley, 2002) package for R to classify the diet of fossil species. The scripts used here were strongly based on the scripts provided by Slater (2015).

In the LDA analysis, two distinct training sets were employed, encompassing extant canids and other carnivores, summing up 35 species. These sets shared the same 25 extant canid species, nine procyonids, and *Ailurus fulgens*, yet were distinguished by different diet classifications. The composition of these training sets mirrored Slater's (2015) methodology, where non-canid species were intentionally included. This choice was motivated by the acknowledgment that fossil canids often exhibit more extreme adaptations to hypocarnivory than observed in their extant counterparts (Wang *et al.,* 1999). The species selected for the training sets were chosen based on their demonstrated effectiveness in the diet classification of fossil species (Slater, 2015), and data availability. These training sets were used to calculate the mean and covariance matrix for each diet category represented within the training set. The dietary categories used were: hypercarnivores, mesocarnivores, hypocarnivores, and herbivores. Using these statistical measures, the LDA model is able to discern the underlying patterns and relationships between craniodental variables and dietary categories. These statistical properties are used to determine the optimal linear transformation that maximizes the discrimination between categories, establishing an association between morphology and dietary categories that are posteriorly used to classify the fossil canids. The two training sets were composed of the same 35 species (25 extant canids and 10 carnivores) with different diet classifications (Supplementary Table 1). The first training set (hereafter, TS1) followed the diet classification proposed by Hopkins *et al.* (2021) with 4 hypercarnivores, 17 mesocarnivores, and 14 hypocarnivores. The second training set (hereafter, TS2) comprised the same 35 species. For TS2, we followed the diet classification provided by Slater (2015), which included 4 hypercarnivores, 6 mesocarnivores, 21 hypocarnivores, and 4 herbivores. The purpose of utilizing these different training sets was to investigate whether the variation between the two sets would impact the ecological classification of the fossil species. By comparing the results obtained from TS1 and TS2, we aimed to assess the robustness and consistency of the ecological classifications in light of different training data and classification schemes.

In the ecological characterization, we utilized craniodental variables to analyze the relationship between morphology and diet. However, since we were unable to impute MAT variable, we conducted two separate discriminant analyses for each training set. In the first LDA, we used the training sets with all six variables to establish the association between the craniodental variables and the different diet categories, generating a multivariate linear model. We assess the accuracy of this model by comparing the original classification of the training set with the one provided by the model. For instance, in TS1 the original classification was 4 hypercarnivores, 17 mesocarnivores, and 14 hypocarnivores. The classification from the model was 4 hypercarnivores, 19 mesocarnivores, and 12 hypocarnivores, representing an accuracy of 94%. For TS2 the accuracy was also 94%. Subsequently, we utilized these trained models by employing the R function *predict ()*. Through this function, we employed the trained LDA model to generate predictions of the dietary categories of the extinct canids. We successfully characterized 61 fossil species. In the second LDA, we excluded the MAT variable (because several fossil species do not have this variable) and followed the same procedure. The accuracy for TS1 was 88%, while the accuracy of TS2, remained at 94%. We applied the trained models for the remaining fossil species and successfully characterized 72 canids. It is important to note that the different training sets resulted in slightly different classifications.

The Training Set 1 (TS1) resulted in 40 hypercarnivores, 80 mesocarnivores, and 13 hypocarnivores, and hence a considerably higher prevalence of mesocarnivores. Conversely, Training Set 2 (TS2) resulted in 36 hypercarnivores, 45 mesocarnivores, and 52 hypocarnivores. Due to the difference observed in the ecological characterization using the training sets and considering that such discrimination procedure is more effective at separating hypercarnivores from the other categories (Van Valkenburgh & Koepfli, 1993; Slater, 2015), we decided to merge mesocarnivores and hypocarnivores, in all subsequent analyses, as non-Hypercarnivores. Hence instead of 3 categories, we ended with 2, Hypercarnivores and Non-Hypercarnivores.

Fossil occurrence data

The compilation and curation of fossil data used in this study were conducted by Lucas M. V. Porto (personal communication). The fossil occurrences from North American canids dataset was compiled from online databases: Paleobiology Database (PBDB; https://paleobiodb.org/#/) and New and Old Worlds fossil mammal database (NOW; https://nowdatabase.org). The curatorial work carried out adopted a conservative measure regarding species taxonomic uncertainty. It kept newly described species identified with "n. sp" but filtered out all occurrences without or with uncertain species identification, removing all occurrences that were tagged with taxonomic uncertainty markers (Bengtson, 1988; Sigovini *et al.*, 2016): "indet.", "Sp.", "?", "Aff.", "Cf.". Faurby *et al.,* (2019) were used to recombine subjective synonyms and subspecies. To remove occurrences with lower temporal resolution, all occurrences with an estimated time interval of more than 6 million years were removed. Given the fossil dataset used is compiled from two distinct databases, it is important to acknowledge the potential presence of duplicates. In this case, duplicates refer to situations where data points are mistakenly treated as independent replicates when they are the same occurrence. This can occur due to overlap or redundancy in the information provided by the databases. It can lead to an overestimation of the sample size and potentially introduce bias into the results. To address the issue of duplication ("pseudoreplication") only fossil occurrences with a temporal range that differed from each other by at least 6 million years and were spatially distant by at least 1 degree in latitudinal and longitudinal coordinates were retained. After all the curatorial work, the final data set was left with 1735 occurrences of 133 species.

Preliminary diversification analyses

To examine the impact of age on the probability of extinction, it is better to conduct diversification analyses within a time interval where the background extinction rate remains constant (Hagen *et al*., 2018). This is crucial because the lifespan of species is inversely proportional to extinction rates (Raup, 1985). Therefore, changes in the background extinction rates could influence lineage duration and interfere with the estimation of age dependency. To establish the appropriate time interval for subsequent analysis, we initially inferred the temporal variation in speciation and extinction rates. This comprehensive analysis encompassed 8 distinct species pools, including those defined by dietary classification (TS1 and TS2) such as Hypercarnivores and Non-Hypercarnivores, as well as those defined phylogenetically such as the entire Canidae family and its three sub-families: Hesperocyoninae, Borophaginae, and Caninae. All analyses were done at the species level.

We employed a birth-death model approach implemented within a Bayesian framework using the software PyRate (Silvestro *et al.*, 2014, 2019) to estimate the diversification rate over time. This model simultaneously estimates: 1- the times of origin and extinction; 2- rates of speciation and extinction; 3- if those rates change through time; 4- the preservation rate, while taking into account several aspects of the incompleteness of the fossil record. The method uses time point estimates for each fossil occurrence, but most fossil occurrences do not have such temporal point estimates but rather a stratigraphic interval defined by upper- and lower-time estimates. To account for age uncertainties in our analyses, we generated 50 replicated resampled datasets for each species pool by randomly sampling a point time within the temporal range of each occurrence, resulting in a total of 400 replicated datasets (50 replicates * 8 different datasets, each representing a different pool of species). Each of these 400 replicated datasets was used in the diversification analysis to describe the temporal trend of diversification rates. Prior to the diversification analysis, we ran a maximum likelihood test to assess which preservation model is best supported by one of those datasets (Silvestro *et al.*, 2019). For all datasets except for non-Hypercarnivores, the model with the lowest AIC was the Time-variable Poisson process (TPP) which allows for shifts in the preservation at 20.43 million years and 4.9 million years or 30.8 million years and 20.3 million years in the Hesperocyoninae analysis. For Non-Hypercarnivores, the best model was a non-homogeneous Poisson process (NHPP). We used the preservations model coupled with a Gamma model, which allowed for preservation rate heterogeneity across lineages. We used a reversible jump Markov Chain Monte Carlo (RJMCMC) to jointly estimate the model parameters, including the number and temporal placement of rate shifts in speciation and extinction (Silvestro *et al.*, 2019). We ran 60 million iterations and sampled once every 10,000 to achieve convergence. The Bayes Factor (Kass & Raftery, 1995) was used to test the evidence in favor of a given temporal shift in diversification rates (speciation or extinction). The effective sample sizes (ESS) were assessed by visualizing the log files in Tracer (Rambaut *et al.,* 2018) after excluding the first 10% of the sample as a burn-in period. All replicas had sufficient sampling (ESS values > 200). From these analyses, we described the general trend in speciation and extinction where we were able to identify the time intervals where the background extinction was constant.

Age-dependency analyses

To infer the degree of age-dependency on extinction rate dynamics we followed the framework described by Hagen *et al.* (2018) and implemented in PyRate. In the age-dependent extinction model (Hagen *et al.*, 2018), lineage duration is modeled according to a Weibull distribution where the shape parameter describes the age-dependence effect on extinction. For a shape parameter > 1, the probability of extinction increases with the age of the taxon; for a shape parameter < 1, the extinction is greater for younger lineages, and it declines with age (Fig. S2). If the shape parameter is equal to or close to 1, then extinction is interpreted to be age-independent, being congruent with the "law of constant extinction" described by Van Valen (1973). In this case, the Weibull distribution reduces to an exponential distribution, which characterizes a simple birth-death model. This framework also explicitly takes into account species that have not been sampled (Hagen *et al.*, 2018). Those are typically short-lived (Foote & Raup, 1996) and their absence could strongly influence our inference of the shape parameter, and hence extinction age-dependency. PyRate deals with this aspect by explicitly modeling how sampling probability relates to species longevities, using the empirical data for that. Hence what is in practice fit to the empirical distribution is not a Weibull distribution *per se* but a modified version that models the potential relationship between sampling probability and species longevities (Hagen *et al.*, 2018). The distribution includes three parameters: the shape and rate of the Weibull (which are used to infer age-dependent extinction), and the preservation rate (which defines how the probability of sampling a lineage varies as a function of its longevity). The joint estimation of these parameters was found to yield unbiased results based on extensive simulations (Hagen *et al.*, 2018). Therefore, in this Bayesian framework, fossil occurrences are used to simultaneously estimate: (1) the "true" times of origination/speciation and extinction of each sampled lineage; (2) the preservation rate for each predefined time window; (3) the parameters of the modified Weibull, including the shape parameter that measures the association between the probability of extinction and the duration of the species.

We ran the age-dependent analysis in each one of the different 14 time windows described (Table 1). In each window, we ran a maximum likelihood test to determine which preservation model is best supported by the data. The age-dependent analysis only allows for the use of the homogeneous Poisson process (HPP) and the time-dependent Poisson process (TPP) models. Therefore, if NHPP was the best model, we selected the second-best model between HPP and TPP. The timespan and the chosen preservation model are summarized in Table 1. The Gamma model was not employed in the age-dependent analysis as it has not been fully tested and preliminary tests showed that in our empirical case, it mistreated singletons when applying the age-dependent model.

Table 1. Window timespan, window name, and preservation model used for each analysis.

Timespan (Mya)	Window Name	Preservation Model
Root age – 6.85 Mya	TS1 Hypercarnivores 01	TPP
Root age – 18 Mya	TS1 Non-Hypercarnivores 01	TPP
14.5 Mya – 0	TS1 Non- Hypercarnivores 02	HPP
Root age – 6.85 Mya	TS2 Hypercarnivores 01	TPP
Root age – 18 Mya	TS2 Non- Hypercarnivores 01	TPP
14.5 Mya – 0	TS2 Non- Hypercarnivores 02	HPP
Root age – 17.6 Mya	Hesperocyoninae 01	TPP
Root age – 7 Mya	Borophaginae 01	HPP
16.75 Mya – 7 Mya	Borophaginae 02	HPP
Root age – 7 Mya	Borophaginae 03	TPP
Root age – 3.5 Mya	Caninae 01	TPP
Root age – 19 Mya	Canidae 01	HPP
17 Mya – 3 Mya	Canidae 02	HPP
Root age – 3 Mya	Canidae 03	TPP

We ran the RJMCMC integrator setting the age-dependency model described for each one of the different 14 time windows described above using 20 million iterations sampled every 10.000 iterations to obtain the posteriors for each parameter. This was done independently for each replica. The ESS was assessed as previously described. With the default parameters of PyRate, we did not reach sufficient sampling, indicated by the effective sample size (ESS) being below 200. To address this issue, we implemented a stricter prior for the shape parameter by changing its standard deviation from 2 to 1 (following Silvestro, personal communication). We compiled the results for all the replicas within a single posterior distribution to summarize the parameter estimation (shape) of the Weibull-modeled distribution of lineage durations in the different species pools. To evaluate the evidence in favor of age-dependent extinction, we compared the 95% highest posterior density (HPD) of the shape parameter of each species pool against the reference value of 1 which defines an age-independent extinction.

The framework used has two key features that influence the estimated parameters: 1 – the duration of each lineage is informed by all of its occurrences; 2 – the method models the unsampled species. In order to explore the impact of unsampled species on the estimation of the age-dependent model, we compared the shape parameter estimated by PyRate (hereafter, PyRate fit) with the shape parameter estimates obtained by directly fitting a Weibull distribution to the estimated longevities of only the sampled species (hereafter, empirical fit). The main distinction between the PyRate fit and the empirical fit lies in the consideration of expected longevities for unsampled species. The empirical fit only utilizes the durations of each sampled lineage (i.e., those with empirical occurrences) estimated after running the age-dependent model, without accounting for the expected longevities of unsampled species. Each longevity was defined as the time interval between the median of the posteriors for the "Time of speciation" and the "Time of Extinction" (estimated using PyRate).

To fit a Weibull distribution in the sampled durations, we used the function *fitdist ()* from the R package *fitdistrplus* (Delignette-Muller & Dutang, 2015). In addition, we conducted a comparison between the Weibull distribution and the exponential distribution to assess the relative evidence of age dependence (Weibull distribution) or independence (exponential distribution). This comparative analysis was motivated by the fact that the exponential distribution is a special case of the Weibull distribution when the shape parameter is equal to 1. For fitting the exponential distribution, we also utilized the *fitdist ()* function. To determine which distribution provides a better explanation for the sampled duration in each species pool dataset, we compared the AIC values. We set a threshold of AIC > 2 to identify the distribution with the better fit.

RESULTS

Preliminary diversification dynamics

We successfully identified time intervals with constant background extinction across all species pools. Our analysis of the two training sets (TS1 and TS2) for hypercarnivores and non-hypercarnivores revealed consistent patterns in extinction rates (Fig. 1 and Fig. S3). Consequently, we have chosen to present only the results from the first training set (Fig. 1). In hypercarnivores (Fig. 1A), the extinction rate remained constant until around 5 million years ago, where we observed a substantial increase in the extinction rate. The Bayes Factors (BF) analysis provided strong support for this rate shift (BF > 6). Following this shift, the extinction rate remained stable until the early Pleistocene, where we observed a shift with less significance (2 < BF < 6). To perform the ADE analysis, we considered a window (TS1 Hyper 01) extending from the period of root age (defined by a 95% HPD between 35.6 and 32.6 million years ago) up until 6.5 million years ago. In the case of non-hypercarnivores (Fig. 1B), the extinction rate remained constant until around 15 million years ago when there was an increase in the extinction rate (2 < BF < 6). Following a period of stability, a potential pulse of extinction occurs in the early Pleistocene, but the evidence supporting it is moderate (2 < BF < 6), and the change in extinction magnitude is small, at least judged by the posterior median. Afterward, the extinction rate remained constant until the present. For non-hypercarnivores, we were able to identify two distinct windows characterized by constant background extinction. The first window (TS1 Non-Hyper 01) spanned from the root age (defined by a 95% HPD between 39 and 37.3 million years ago) until 18 million years ago, while the second window (TS1 Non-Hyper 02) extended from 14.5 million years ago to the present.

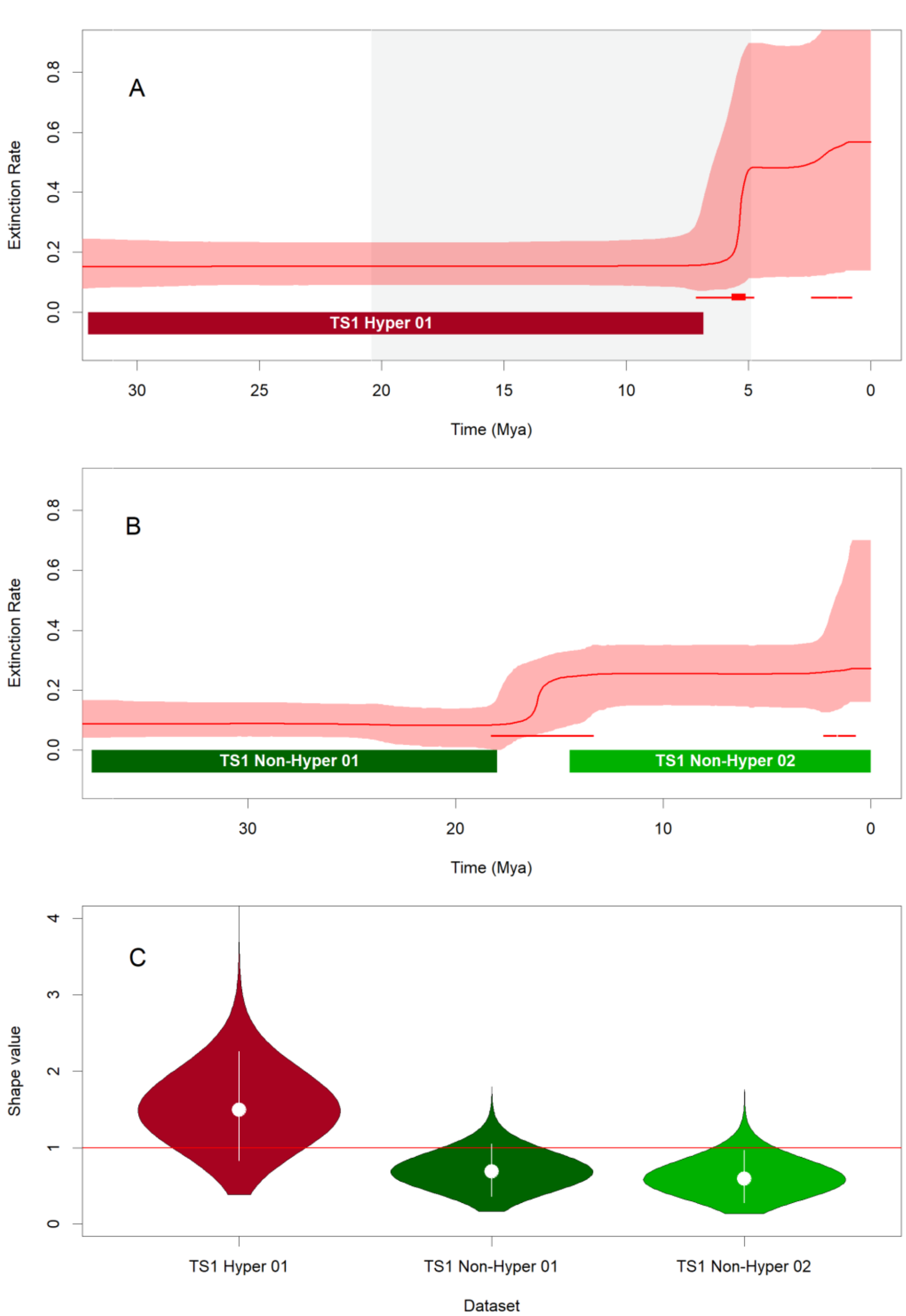

Figure 1. Extinction rate and age-dependency in hypercarnivores and non-hypercarnivores for the first training set (TS1). Panels A and B display plots of extinction rates over time, with the light-colored area representing the 95% highest posterior density interval (HPD) for the extinction rate of hypercarnivores (panel A) and non-hypercarnivores (panel B). The solid line within the light-colored area represents the median of the posterior distribution of rate values at each time point. Red horizontal segments indicate times of low significance (2 < BF < 6) rate shifts in extinction, while red rectangles mark times of highly significant (BF > 6) rate shifts in speciation and extinction. In panel A, the white and grey background bars indicate the preservation intervals used in the analysis, allowing preservation to vary among but

remain constant within intervals. Colored horizontal bars indicate the length of the different time windows used in each ADE analysis. Panel C presents violin plots, combining the posterior distribution for the shape parameter of the Weibull distribution for each time window. The vertical white lines in panel C represent the 95% HPD, and the white dot indicates the median of each posterior distribution. The red horizontal line indicates age-independency (shape value = 1).

We examined the changes in extinction rates for the Canidae family and its three subfamilies (Hesperocyoninae, Borophaginiae, and Caninae) (Fig. 2). For Hesperocyoninae (Fig. 2A), the extinction rate remained constant until a shift with moderate support (2 < BF < 6) occurred approximately 18 million years ago resulting in a moderate increase in the extinction rate. We established a single time window (Hesperocyoninae 01) extending from the root age (defined by a 95% HPD between 37.4 and 36.8 million years ago) to 17.6 million years ago. In the Borophaginae subfamily (Fig. 2B), the extinction rate, remained constant until 15 Ma when a shift in the extinction pattern occurred (2 < BF < 6), resulting in a mild increase. After another period of stability, there was another significant (BF > 6) increase in extinction at the Miocene/Pliocene boundary. Yet another shift in the extinction rate took place during the early Pleistocene (2 < BF < 6). For the Borophaginae, we have identified three distinct time windows. The first window, Borophaginae 01 encompasses the time from the root age (defined by a 95% HPD between 35.6 and 33.4 million years ago) to 16.75 Ma. The second window, Borophaginae 02, covers the period from 16.75 Ma to 7 Ma. Lastly, the third window, Borophaginae 03, spans from the root age (defined by a 95% HPD between 35.6 and 33.4 million years ago) to 7 Ma. In the Caninae subfamily, the extinction rate remained stable until the late Pliocene, at which point we witnessed a low-significant shift (2 < BF < 6) leading to an increase in the extinction rate (Fig. 2C). We have identified a single time window, (Caninae 01) which covers the timeframe from the root age (defined by a 95% HPD between 32.2 and 28.6 million years ago) to 3.5 Ma (Fig 2C). In the case of Canidae (Fig. 2D), a low-significant shift (2 < BF < 6), pertaining small change in the magnitude of extinction, was identified around 20 million years ago. Following a period of stability, the extinction rate exceeded the speciation rate during the early Pliocene, with another increase in extinction around the Pliocene/Pleistocene boundary. Both of these shifts show moderate support (2 < BF < 6). For Canidae, analyses were conducted within three distinct time windows. The first window (Canidae 01) extended from the root age (defined by a 95% HPD between 37.5 and 36.9 million years ago) to 19 million years ago. The second window (Canidae 02) covered the period from 17 million years ago to 3 million years ago. Lastly, the third window (Canidae 03) encompassed the time from the root age to 3 million years ago. This last Canidae window was chosen to evaluate the effect of allowing a small change in extinction value while allowing more data to be analyzed at the same time.

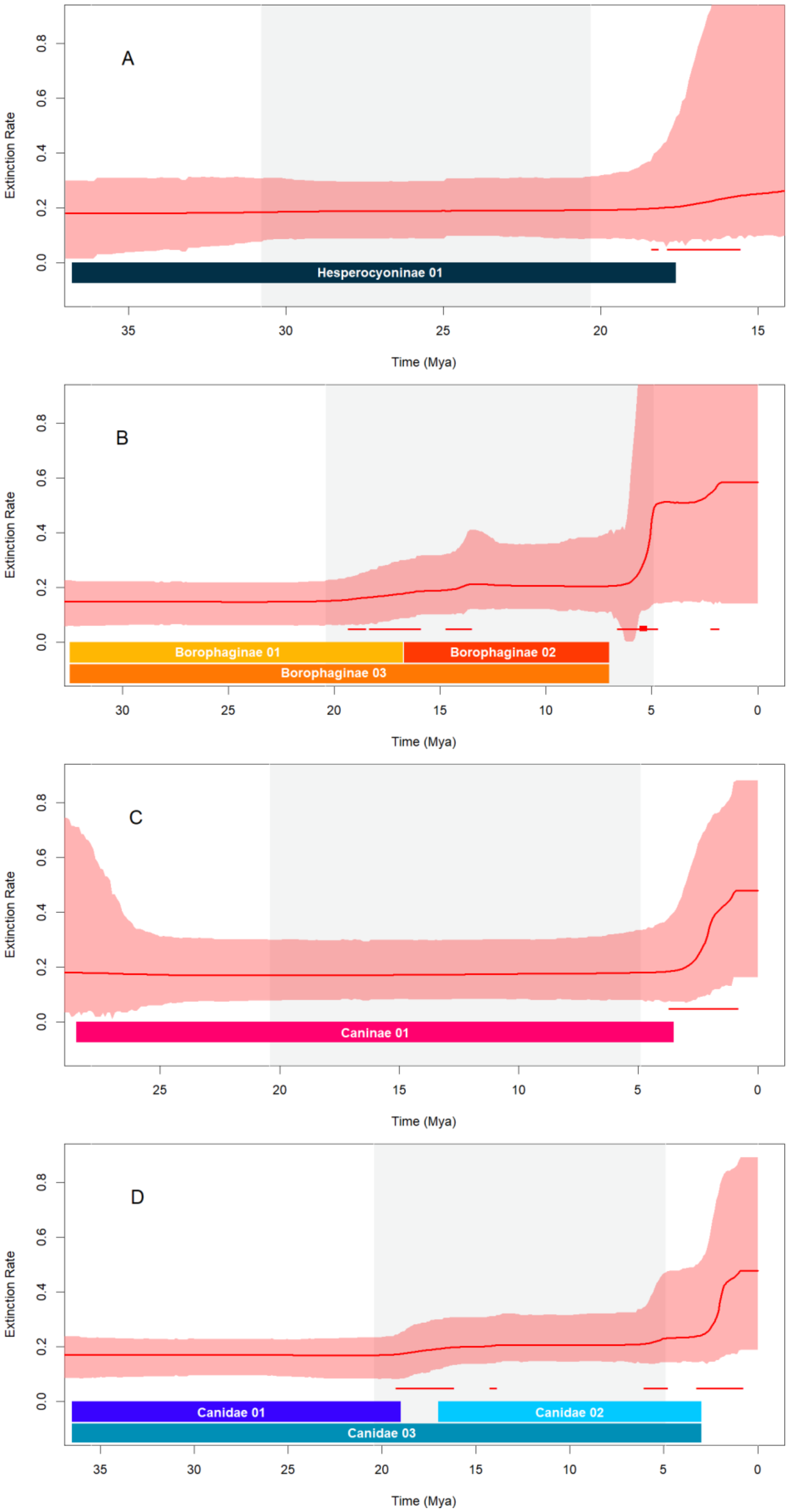

A
Hesperocyonínae 01
B
Borophaginae 01
Borophaginae 02
Borophaginae 03
C
Caninae 01
D
Canidae 01
Canidae 02
Canidae 03
Extinction Rate
Time (Mya)

Figure 2. Extinction rate through time for Canidae and its subfamilies. Panels A, B, C, and D show rate through time (RTT) plots, with the light-colored area representing the 95% highest posterior density interval (HPD) for extinction (red) rate for Hesperocyoninae (Panel A), Borophaginae (Panel B), Caninae (Panel C), and Canidae (Panel D). The continuous line inside the light-colored area indicates the median of the posterior distribution of rate values at each moment in time. Red horizontal segments signify times of low significance ($2 < BF < 6$) rate shifts in speciation and extinction rates, while red rectangles represent the times of highly significant ($BF > 6$) rate shifts in extinction. The white and grey background bars indicate the preservation intervals used in the analysis where we allowed preservation to vary among but be constant within intervals (preservation variation among lineages was allowed within each time window). The horizontal colored bars on the bottom of panels (A), (B), (C), and (D), indicate the length of the different time windows used in each ADE analysis.

Age-dependent analysis

Our analysis reached sufficient sampling (ESS > 200) in all windows for each one of the different species pool datasets. Our findings from TS1 and TS2 were generally consistent, except for the first window of non-hypercarnivores (compare TS1 Non-Hyper 01 in Fig. 1C to TS2 Non-Hyper 01 in Fig. S3C). Although we discuss this difference, we present only the results from TS1 here, but the results from TS2 are available in the supplementary material. In our analysis of hypercarnivores, we found moderate evidence in favor of a positive age-dependent extinction at the TS1 Hyper 01 window. This is because the 95% HPD (Highest Posterior Density) interval estimate for the shape parameter (median = 1.5, 95% HPD = 0.79 – 2.23) includes the value of 1 (Fig. 1C). However, it is worth noting that there is a suggestive trend towards positive age-dependent extinction. When visually inspecting the shape estimates for each replicated dataset individually (Fig. S5), we observe that all replicates show their posterior shifted toward values higher than 1, with a few replicated datasets providing strong evidence for positive age dependency.

In the non-hypercarnivores, we identified strong evidence of negative age dependency in one window and moderate to strong in the other. In the TS1 Non-Hyper 01 window (Fig. 1C), although the 95% HPD interval for the shape parameter (median = 0.69, 95% HPD = 0.37 – 1.05) still crosses the value of 1, the expectation for age-dependency extinction, there was a clear tendency towards negative age-dependency. However, in the TS2 Non-Hyper 01 window (Fig. S3C), this result was quite different, and we found strong evidence for age-independent extinction, as the shape parameter was very close to 1 (median = 0.93, 95% HPD = 0.5 – 1.41). Both windows cover the same period, with the only difference being the presence of four additional species being classified as non-hyper carnivores in TS2 Non-Hyper 01 (*Cynodesmus thooides, Mesocyon brachyops, Paraenhydrocyon wallovianus,* and *Sunkahetanka geringensis*). Those were classified as hypercarnivores in TS1. Based on previous works that classified these species as hypercarnivores (Van Valkenburgh, 1991; Wang, 1994; Van Valkenburgh *et al*., 2004; Holliday & Steppan, 2004; Slater, 2015) we believe that the classification as hypercarnivores is more adequate, but we note some authors have classified at least one of these species as non-hypercarnivores (Holliday & Steppan, 2004; Balisi & Van Valkenburgh, 2021). In the TS1 Non-Hyper 02 window (Fig. 1C), we observed a clear strong signal for negative age-dependency. The estimated shape parameter of the Weibull distribution (median = 0.59, 95% HPD = 0.29 – 0.96) was significantly smaller than 1, providing strong evidence for negative age dependency in this window. The presence of a negative age-dependency trend in both windows (TS1 Non-Hyper 01 and 02) becomes evident when examining the estimated shape values for each replicated dataset individually within this time window (Fig. S6 – S7). Several of the individual replicated datasets demonstrate strong evidence for negative age dependency.

Our analysis of the phylogenetic species pool, which includes Canidae, Hesperocyoninae, Borophaginae, and Caninae, suggests a scenario in accordance with age-independency extinction (AIE) for most time windows (Fig. 3). The 95% HPD interval of the shape parameter crosses 1 for all analyses, but there is some considerable variation among the different windows. In Hesperocyoninae 01 (Fig. 3A), we observe a wide posterior distribution, with a positive median close to 1 (median = 1.19, 95% HPD = 0.55 – 1.97). Upon visually inspecting the replicated datasets, we notice that several replicated datasets suggest strong evidence for age independence since most posterior estimates are centered closer to 1, while others indicate weak evidence in favor of positive age dependency (Fig. S11). In the three windows of Borophaginae, we notice a weak tendency towards positive age-dependent extinction (Fig. 3A), but the posterior distribution of the shape parameter crosses 1 in all three windows: Borophaginae 01 (median = 1.34, 95% HPD = 0.63 – 2.24), Borophaginae 02 (median = 1.47, 95% HPD = 0.75 – 2.31), and Borophaginae 03 (median = 1.35, 95% HPD = 0.97 – 1.76). When we visually inspect the replicated datasets for Borophaginae 01, the posterior distribution of all replicated datasets crosses the value of 1, but at different percentiles (Fig. S12). In Borophaginae 02, we observe similar patterns, but a few replicated datasets provide strong evidence for positive age dependency (Fig. S13). In Borophaginae 03, all replicates show their posterior shifted towards values higher than 1, with some replicated datasets providing compelling evidence for positive age dependency (Fig. S14). We note the Borophaginae 03 time window encompasses a rate shift in extinction, which might influence the estimates of the shape parameter. Conversely, Caninae 01 (median = 0.70, 95% HPD = 0.30 – 1.20), exhibited a weak tendency towards negative age-dependent extinction (Fig. 3B). Upon visual inspection of the replicated datasets, we can see that all replicates show their posterior distributions shifted towards values lower than 1, with some replicated datasets providing evidence for negative age-dependency (Fig. S15). In Canidae (Fig. 3B), the shape parameter for each window was found to be very close to 1: Canidae 01 (median = 0.84, 95% HPD = 0.45 – 1.24), Canidae 02 (median = 0.96, 95% HPD = 0.59 – 1.38), and Canidae 03 (median = 1.15, 95% HPD = 0.89 – 1.44). By visually examining the replicated datasets of Canidae 01 and Canidae 02, we notice that in several replicated datasets, most posterior estimates are centered close to 1, which supports age independence (Fig S16 - S17). In Canidae 03, we found some support for a positive age dependency in some replicates, while at the same time, we have support for age independence (Fig. S18). We note this time window encompasses a rate shift in extinction. It is interesting to note that both longer windows analyzed here (Borophaginae 03 and Canidae 03) that include a shift in extinction result in a shape value higher than 1.

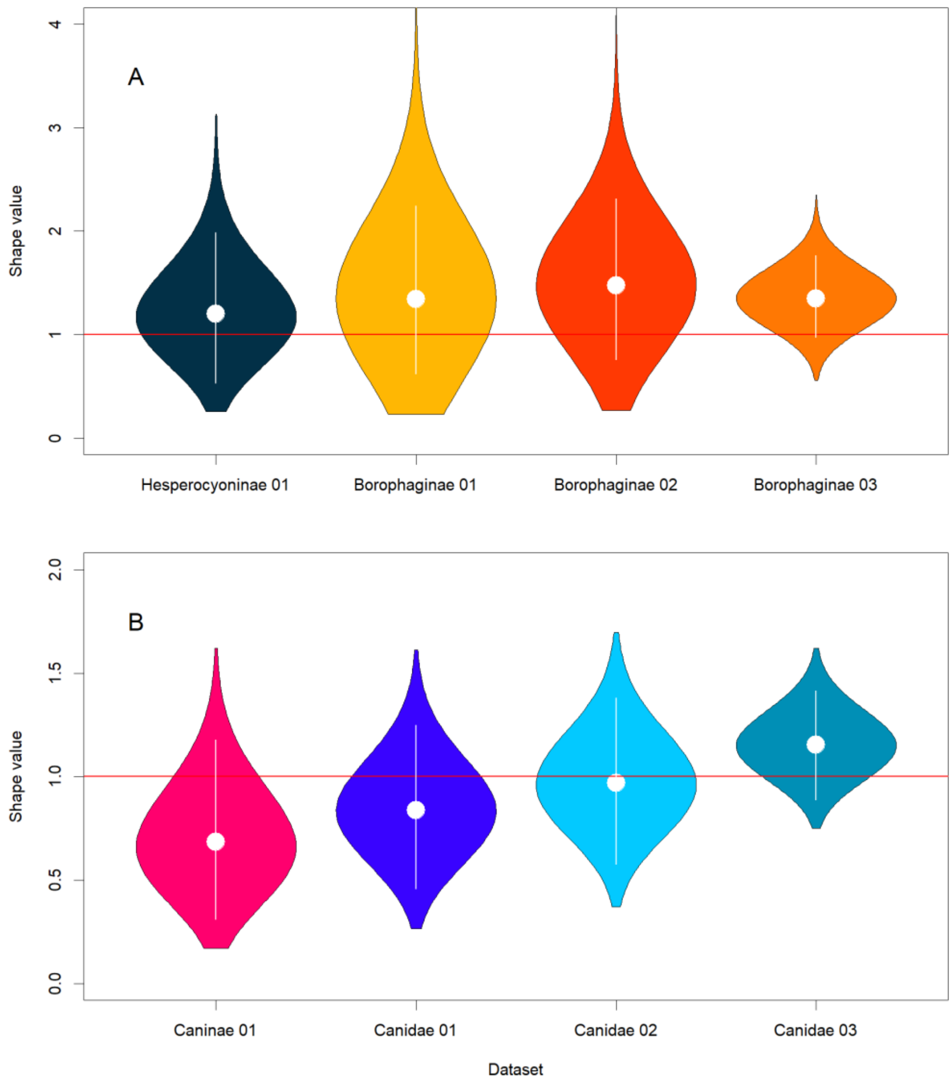

Figure 3. Extinction age-dependency for Canidae and its subfamilies. Panels A and B display violin plots representing the combined posterior distribution for the shape parameter in the Weibull distribution for each time window. The vertical white lines in the panels indicate the 95% highest posterior density (HPD) interval, and the white dot represents the median of each posterior distribution. The red horizontal line indicates age-independency (shape value = 1).

The empirical fit analysis results when using only sampled species align well with the PyRate analysis, with only a few exceptions (Fig 4). In most cases the interpretation of whether a given pool better fits the AIE or ADE was similar, one notable exception would be for non-hypercarnivores. In the analysis of non-hypercarnivores, the exponential distribution showed a better fit than the Weibull in most replicated datasets (proportion of replicated datasets with a better fit on exponential: TS1 Non-Hyper 01 = 96%; TS1 Non-Hyper 02 = 100%). This suggests age-independent extinction dynamics, while visual inspection of the posterior distribution would suggest evidence in favor of negative age dependence. These findings indicate that the inference of independent or dependent extinction is significantly influenced by the presence of unsampled species, and to a lesser extent by the approach used and how we interpret their results. It is also worth noting that in all replicated datasets, the shape parameter values obtained from the empirical fit of sampled species were, as expected, always higher than the median values obtained from the PyRate analysis.

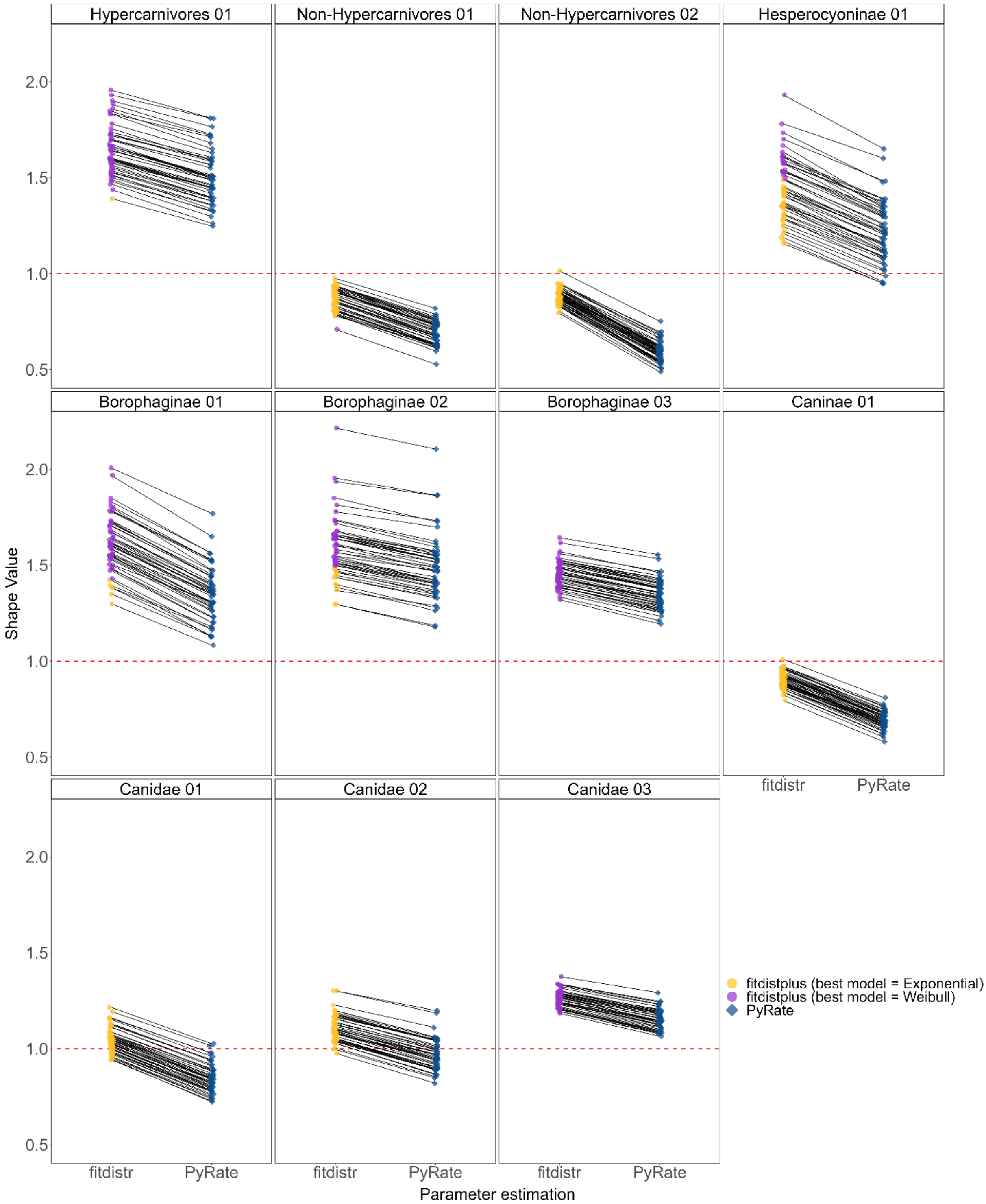

Figure 4. Estimates of Weibull shape for each replicated dataset using PyRate's Age-dependence extinction model are represented by blue diamonds (median values), while circles depict estimates obtained through *FitDistrPlus*, considering only sampled species in each time window. Purple circles indicate replicated datasets that were better adjusted to a Weibull distribution, and yellow circles refer to replicated datasets that were better adjusted to an Exponential distribution. The red horizontal line represents age-independency (shape value = 1). Shape estimates from the same replicate from the same dataset are connected by black lines.

To help visualize the interplay between the different ways to create the species pool (by diet or phylogeny), the heterogeneity among replicates, and the effect of missing species, we plotted the empirical longevities and the expected Weibull curve for each individual replicate (red lines in Fig. 5 and Fig. 6). These curves were constructed using the shape and scale derived from PyRate's age-dependent model, superimposed over the empirical distributions of species longevities which were color-coded according to their phylogenetic affiliation (histograms in Fig. 5) or diet (Fig. 6). For both hypercarnivores and non-hypercarnivores, the vast majority of estimated curves fit visually well with the distribution of empirical longevities (Fig. 5). We observe some shape variation in hypercarnivores, as evident in the differences in the Weibull curves (red lines in Fig. 5A), but there is an overall tendency for positive age-dependent extinction (also evident from figure S5), suggesting most PyRate analysis did not inferred that several species with short durations were missing (note low abundance of short-lived sampled species). We also see that within the studied time window, the hypercarnivore pool is solely composed of Hesperocyoninae and Borophaginae species. In contrast, for non-hypercarnivores in both time windows, we see less variation in the shape estimate and the presence of species from the Caninae sub-family, in particular in the second time window where they are the vast majority (Fig. 6B – C). When analyzing the subfamilies, we see significant variation in the estimates for hesperocyoninae (Hesperocyoninae 01) and two windows of the borophaginae subfamily (Borophaginae 02 and 03). This variation appears to be supported by the analysis of several replicates, which suggests that species with very short longevities were not sampled, indicating that the preservation model behaved quite differently across the different datasets. However, even with the larger variation observed in the borophaginae analysis, both the empirical distribution and most of the estimates indicate a tendency for positive age-dependent extinction. We also see that, except for Borophagina 01 and Caninae 01 time windows, which have only non-hypercarnivores, all time windows showed both hyper and non-hypercarnivore species.

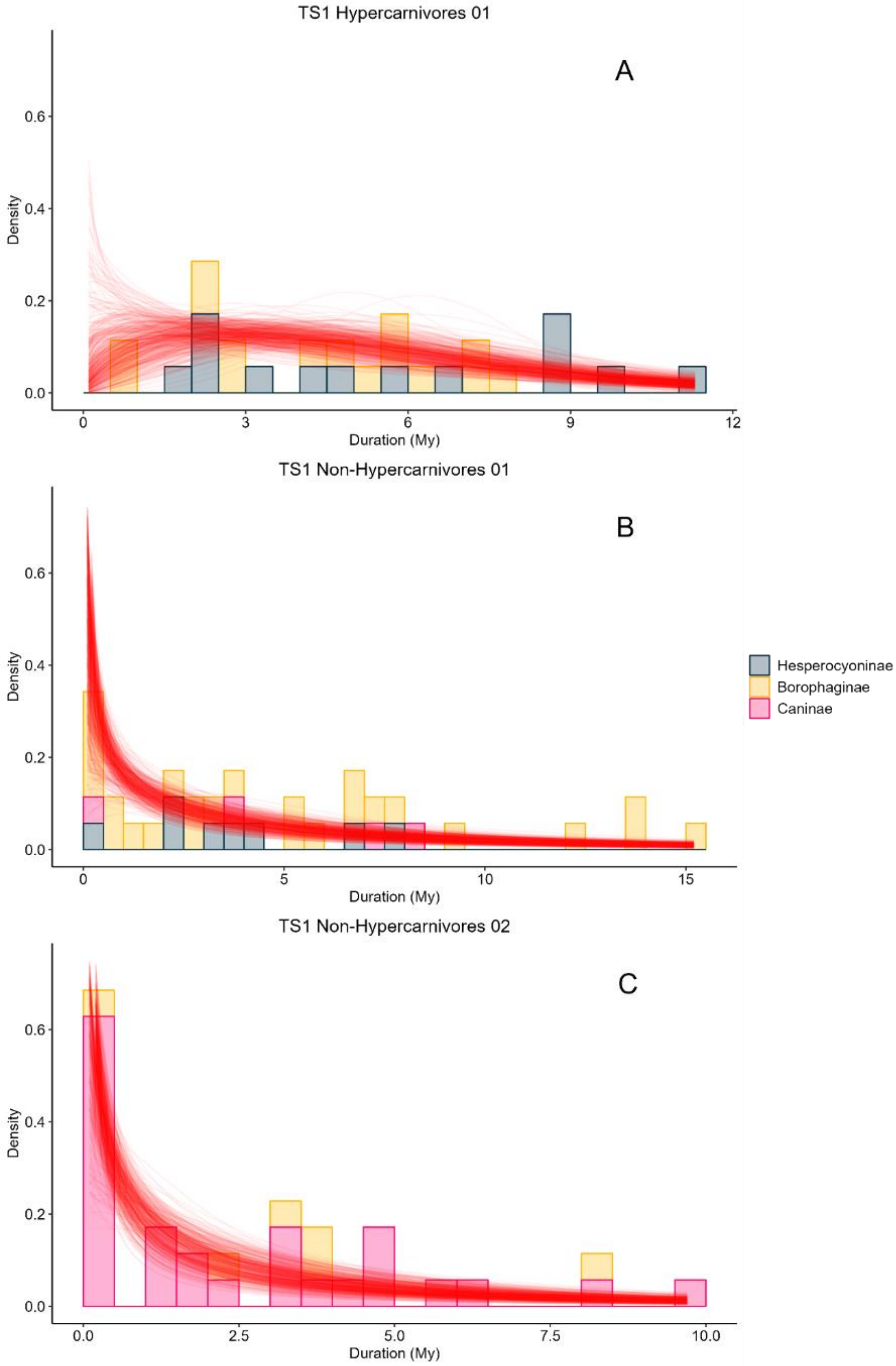

Figure 5. Empirical distribution of species durations estimated in PyRate for the sampled taxa and age-dependent model results. Empirical longevity estimates were taken for the combined posterior distribution using all replicates by taking the difference between the estimated median values for the times of speciation and extinction. The color bars in all panels indicate the different Canidae subfamilies (Blue: Hesperocyoninae, Yellow: Borophaginae, and Pink: Caninae). Panel A shows the TS1 Hypercarnivores window, Panel B shows the TS1 Non-Hypercarnivores window, and Panel C

shows the TS1 Non-Hypercarnivores window. For each panel, the Weibull distributions estimated for different iterations by PyRate's age-dependent model are illustrated using 500 semitransparent red lines, which are randomly drawn from the combined posterior.

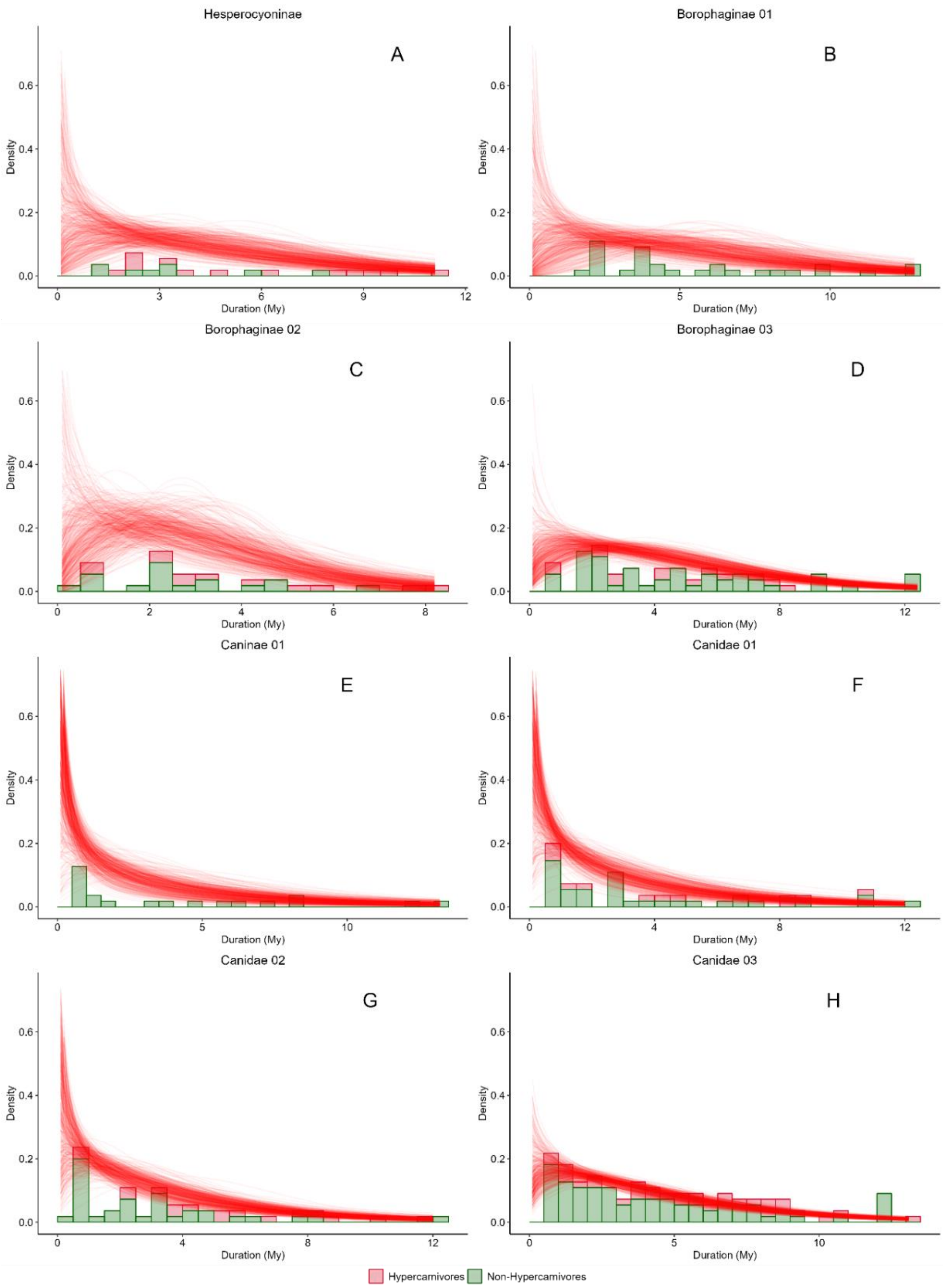

Figure 6. Empirical distribution of species durations estimated in PyRate for the sampled taxa, and the results for the age-dependent model at each window. Empirical longevity estimates were taken for the combined posterior distribution using all replicates by taking the difference between the estimated median values for the times of speciation and extinction. In all panels, the color bars indicate the diet

categories of Canidae (Pink: hypercarnivores, and Green: non-hypercarnivores). Panel A shows the Hesperocyoninae 01 window, panel B shows the Borophaginae 01 window, panel C shows the Borophaginae 02 window, panel D shows the Borophaginae 03 window, panel E shows the Caninae 01 window, panel F shows the Canidae 01 window, panel G shows the Canidae 02 window, and panel H shows Canidae 03 window. Within each panel, the Weibull distributions estimated for different iterations by PyRate's age-dependent model are depicted using 500 semitransparent red lines, randomly drawn from the combined posterior.

DISCUSSION

Here we investigated how different species pools defined by ecology or phylogeny (taxonomy) interfere with our inference of the "Law of Constant Extinction". We demonstrated that species pools defined by phylogeny and ecology exhibit different age-dependent extinction dynamics. In the ecological pool of species, different guilds showed distinct patterns of age-dependent extinction. Furthermore, within the Canidae family, which encompasses different ecological categories (i.e., Hypercarnivores and Non-hypercarnivores), we observe that different phylogenetic pools, either in the same taxonomic rank (different sub-families) or at different ranks (family vs. subfamily) showed distinct patterns of age-dependent extinction.

We found different signals of age-dependent extinction when using different species pools defined by phylogeny or ecology (Fig. 1 and Fig. 3). While the evidence is not overwhelming, as some analyses suggest age-independent extinction, a significant portion of our ADE (Age-dependent extinction) analyses support the presence of age-dependent extinction across most time intervals. When using the phylogenetic species pool, our results revealed a spectrum of signals concerning age dependency or age-independency in extinction patterns. Some analyses have provided compelling evidence for negative age-dependent extinction (notably observed in Caninae 01 and Canidae 01), while others have pointed to weaker evidence in favor of a positive age-dependent extinction (as evident in Borophaginae 01, Borophaginae 02, Borophaginae 03, and Canidae 03). Additionally, there are instances where evidence strongly supports age-independent extinction as is the case of Canidae 02.

In our analysis of the phylogenetic species pool, the different pools also represent not only different clades but also nested pools, here represented by the use of different taxonomic levels (family vs. subfamily). While the different subfamilies showed opposing signals with Borophaginae and Hesperocyoninae showing positive shape values and Caninae showing negative values, the whole family showed a signal more akin to age-independent extinction, in particular the Canidae 02 time window. In a previous study on carnivores, a negative age-dependent extinction was identified at the Order level (Hagel *et al*., 2018). Hence the age-dependent signal might shift from positive (Borophaginae 02), to age-independent (Canidae 02), to negative (whole Carnivora – Hagen *et al*., 2018) depending on the taxonomic rank used to delimit the species pool. Additionally, we might or not observe changes in the age-dependent signal for the same taxonomic pool of species at different time windows. Within the Canidae family, we have observed distinct signals of age-dependency across different time intervals, aligning with similar observations made by Crampton *et al*. (2016), who showed that the signal of age-dependent extinction might change over time. On the other hand, the age-dependent signal for the Borophaginae subfamily, is similar across different time intervals, remaining consistently positive. The variability in the signals of age-dependency across different taxonomic ranks and among different time windows confirms the expectation that the pool of species strongly influences the age-dependent signal of extinction and invites one to think about what those differences mean and how the ecological composition within each phylogenetic defined pool of species might interfere with our inference.

Even though hypercarnivory evolves in all three Canidae sub-families, it is more predominant in the Hesperocyoninae and Borophaginae subfamilies. While those two subfamilies have 14 and 20 hypercanivorous species out of 23 and 68, Caninae only has 6 hypercanivorous species out of 42 species. In our time windows we have: 0 hyper out of 28 in the time window Borophaginae 01, 12 hyper out of 29 in the time window Borophaginae 02, 13 hyper out of 21 in the time window Hesperocyoninae 01, and not a single hypercarnivore in time window Caninae 01. Although not perfect (but see discussion below), we see a tendency for those phylogenetic species pools that contain more hypercarnivores to be more likely to present positive-age dependency. Given the different tendencies regarding the age-dependent signal, it is indeed possible that ecology is determining how age affects the probabilities of extinction.

Notably, in the ecological species pool, our findings reveal evidence of positive age-dependent extinction among hypercarnivores and negative age-dependent extinction among non-hypercarnivores. A very similar dynamic emerged in our second training set, except for the analysis for TS2 Non-hypercarnivores 01, where we detected evidence for age-independent extinction. Interestingly, the only distinction between TS1 Non-hypercarnivores 01 and TS2 Non-hypercarnivores 01 is the inclusion of four species categorized as hypercarnivores in the TS1 as non-hypercarnivores in the TS2 Non-Hypercarnivores 01 analysis. Their classification as hypercarnivores, used in TS1, is more consistent with previous studies (Van Valkenburgh, 1991; Wang 1994; Van Valkenburgh *et al*., 2004; Holliday & Steppan, 2004; Slater, 2015). This suggests that these four hypercarnivore species might be influencing the inference in TS2, potentially skewing it toward a more positive age-dependent extinction pattern.

We note that the age-dependent extinction signal observed when using the ecological pool of species helps us explain the different signals we found when using the phylogenetic. While this finding does partially support our initial hypothesis that different species pools would yield distinct signals, it also contradicts our expectation that the ecological pool would exhibit a stronger age-independent signal compared to the phylogenetic pool. In this context, sub-families with a higher proportion of hypercarnivores (Borophaginae and Hesperocyoninae) displayed fewer positive estimates of the shape parameter compared to the hypercarnivore pool of species. In contrast, the Caninae subfamily, with the lowest proportion of hypercarnivores, revealed a shape parameter estimate that does not exhibit as pronounced a negative trend as the non-hypercarnivore species pool. One important exception is the result for Borophaginae in window 01, which displayed a significantly positive shape parameter value, despite the absence of any hypercarnivore species in that time window. It is interesting to note that the Borophaginae 01 time window has a very high proportion of mesocarnivores, 18 out of 24 (and hence very few hypocarnivores), some of which might have quite similar diets to hypercanivores. This highlights a potential limitation in using diet categories to define the species pool, especially when inferring the diet of extinct species is challenging. In accordance with the ecological species pool reasoning, we also note that the Borophaginae 02 time window showed a much stronger signal of positive age-dependent extinction and a higher proportion of hypercarnivores in that pool.

Our original expectation was to find a stronger signal of negative age dependency for hypercarnivores, the exact opposite of our results (Fig. 1). The rationale behind the phenomenon of negative age-dependent extinction is typically attributed to population size and geographical range (area) dynamics (see also Saulsbury *et al*., 2023 for a mechanistic model). According to this explanation, newly formed species typically originate within a highly constrained geographical range and possess small population sizes (Vrba, E. S. & DeGusta, 2004; Rosenblum *et al*., 2012). However, as these species age, their geographical ranges and population sizes tend to expand (Miller, 1997; Liow & Stenseth, 2007; Kiessling & Aberhan, 2007), resulting in a lower vulnerability to extinction (Payne & Finnegan, 2007; Foote *et al*., 2008; Jablonski, 2008). Another possible explanation centers on the development of traits that provide resistance to extinction, as a generalist ecological niche, potentially leading to age-dependent patterns, or in a higher-level filtering mechanism that filters out clades more likely to go extinct, a mechanism known as the "Extinction filter hypothesis" (Balmford, 1996). This highlights one important aspect raised by Finnegan *et al*. (2008), the decline in extinction rates as lineages age could result from an overall increase in the "fitness" within each lineage, either through anagenesis or via higher-level selection (in a broad sense) against "less fit" lineages. Additionally, Smits (2015) presented compelling evidence suggesting that during the Cenozoic era, generalist species among North American mammals had a lower probability of extinction. This finding suggests that traits conferring resistance to extinction may have evolved and been positively selected. Our findings indicate that non-hypercarnivores may be more susceptible to these mechanisms than hypercarnivores, contrary to our initial hypothesis.

Although hypercarnivores typically have lower population densities (Van Valkenburgh *et al*., 2004), which presumably lead to a higher extinction rate (Purvis *et al.*, 2000), in particular when new species emerge, they are also expected to have large geographical distributions that typically decrease the probability of extinction (Van Valkenburgh *et al*., 2004; Payne & Finnegan, 2007; Foote *et al*., 2008; Jablonski, 2008). A larger geographical distribution and large body size might indicate a higher dispersal rate (Hoekstra & Fagan, 1998) which would allow them to quickly escape the initial stages of a higher probability of extinction and induce an extinction regime dictated by other factors that more strongly affect older species.

Even though positive ADE may be an artifact produced by an increase in the chance of pseudo-extinction as species get older (Doran *et al*., 2006), positive age-dependent extinction patterns have been attributed to general evolutionary ratchet mechanism leading to "species senescence" and lower evolvability (akin to the ratchet process described by Muller, 1964), and the evolution of specialization (Pearson, 1995). Those hypotheses typically evoke evolutionary changes happening within a given species, not among species, as the most important underlying factor. To explain positive-age dependent extinction, some authors have emphasized specific scenarios such as the absence of evolutionary novelty (Condamine *et al*., 2021), and the inability to adapt in response to a changing environment (Jouault *et al*., 2022).

In Canidae, there is a negative association between dietary specialization and species duration (Van Valkenburgh *et al*., 2004; Balisi & Van Valkenburgh, 2018). While the evolution of larger body size and carnivorous tendencies may confer advantages at the individual level (Griffiths, 1980; Carbone *et al*., 2007; Rasmussen *et al*., 2008), it can lead to a macroevolutionary ratchet effect (Van Valkenburgh *et al*., 2004, but see Balisi & Van

Valkenburgh 2020), leading hypercarnivory to evolve repeatedly and independently among unrelated lineages (Van Valkenburgh, 2007). In Hesperocyoninae and Borophaginae, these lineages are initially small-bodied forms but eventually transitioned into species showing larger sizes, and with hypercarnivorous diets before ultimately facing extinction (Van Valkenburg *et al*., 2004; Sorkin, 2008). This evolutionary trajectory suggests the presence of a macroevolutionary ratchet effect, where large body size and dietary specialization, coupled with reduced population densities, heightened the risk of extinction (Van Valkenburgh *et al*., 2004; Van Valkenburgh, 2007). Although hypercarnivory might increase extinction risk, we note that such "macroevolutionary ratchet" might not be sufficient to explain positive age dependence. It is also important to note that the term "macroevolutionary ratchet" is used in a slightly different way as the "general evolutionary ratchet mechanism" proposed to decrease evolvability at the species level. The former evokes an idea of higher-level selection in a broad sense, while the second is typically discussed as a microevolutionary phenomenon that increases the extinction risk within a species as it ages. Under this reasoning, if hypercarnivore species continue to evolve towards higher specialization, a classic anagenetic scenario, then the evolution of specialization might potentially help to explain the positive ADE.

Hypercarnivore adaptations which include the simplification or loss of dental structures (Holliday & Steppan, 2004; Van Valkenburgh, 2007) exemplify Dollo's law. According to this law, once a structure is lost (or changed to another very different state), it is unlikely to be regained (or reverted to the ancestral state) (Holliday & Steppan, 2004). Specialists with modified and simplified characteristics give fewer opportunities for evolutionary changes and a restricted range of possible adaptations for descendent species than generalists who preserve ancestral morphology (Vermeij, 1973). Over macroevolutionary timescales, it appears that canids frequently follow a unidirectional path toward large body size and increasing specialization, with reversals being rare or non-existent (Van Valkenburgh *et al*., 2004; Holliday & Steppan, 2004). Using a phylogenetic approach, Slater (2015) showed that for Canidae, there is not a single reversal from hypercarnivores to non-hypercarnivores. Consequently, the evolution of hypercarnivory and large body size tends to elevate the prevalence of dietary specialization in the later stages of a clade's history, often culminating in the clade's eventual disappearance (Van Valkeburgh *et al*., 2004). Within the carnivore group, the combined factors of the difficulty of reversal and selection for larger size and hypercarnivory act like a macroevolutionary ratchet (Van Valkenburgh, 1999). This macroevolutionary ratchet effect limits the future diversity of a clade as its member species progressively become larger, more specialized, and less abundant (Viranta, 2004; Van Valkenburgh *et al*., 2004). Additionally, Holliday & Steppan (2004) found that hypercarnivores faced more pronounced limitations in their subsequent morphological evolution compared to less specialized forms. Their research strongly indicates that as taxa evolve towards hypercarnivory, the degree of morphological flexibility undergoes a significant reduction relative to a more generalist form. Consequently, specialists like canids hypercarnivores may exhibit reduced evolvability (Kirschner & Gerhart, 1998; Wagner, 2008), narrowing their capacity to respond to environmental changes and selection pressures over evolutionary timescales.

The scenario and mechanisms discussed above exemplify a higher-level selection against hypercarnivory and most of our current knowledge of the effect of hypercarnivory (or trait evolution in general) on extinction rates, as discussed above, evolves the comparison among species. Much less is known about how the evolution of such traits within a given species might impact its probability of extinction as the species ages. Contrasting the lower and higher-level mechanisms through the lens of different species pools (phylogenetic vs ecological) might help our understanding of the likelihood of ratchet and specialization mechanisms being the underlying mechanisms producing positive ADE for hypercarnivores.

The evolution of hypercarnivory could set the stage for a stronger "arms race" with their prey (as opposed to the non-hypercarnivores) leading to an increase in specialization and potentially lower evolvability as species age. Unfortunately, the fossil record is not complete enough to allow us to track such morphological trajectory within species, not allowing such anagenetic mechanism to be properly studied. That said, the temporal trend in body size and specialization described for the Canidae clade (Van Valkenburgh *et al*., 2004; Silvestro *et al*., 2015), the suggestion that hypercarnivory leads to a higher extinction rate (van Valkenburgh *et al* 2004; but see Balisi & Van Valkenburgh 2020), and the lack of re-evolution of non-hypercarnivores (Slater, 2015), seem to undermine the anagenetic mechanisms as potentially relevant explanations to the positive ADE seen in hypercarnivores described here. As the diversification unfolds and new hypercarnivore species emerge, especially if they exhibit an even higher degree of hypercarnivory compared to their ancestral species (Van Valkenburgh *et al*., 2004), the effect of hypercarnivory on extinction risk would if anything, increase its risk of extinction for newly produced species. Because those would also be the younger species in the pool of species, this macroevolutionary effect of hypercarnivory would tend to produce either a negative ADE or AIE. This suggests that other mechanisms are at play here. Pearson (1995) reaches similar conclusions about the implausibility of a "senescence" mechanism as a potential explanation for positive ADE in planktonic foraminifera, trilobites, condonts, and graptolites, raising the possibility that in fact factors extrinsic to the species themselves, such as environmental change, might strongly contribute to generating positive ADE patterns.

We also note that the hypotheses concerning negative age-dependent extinction (e.g., lower population sizes and geographical distributions) are typically centered on ecological factors (demographic and/or area effects), not evolutionary changes, as those proposed by positive age-dependent mechanisms (e.g., evolutionary ratchet mechanisms and lack of evolvability). We suspect that ecologically driven mechanisms might also be at play for Canidae species in North America. Recent unpublished preliminary analysis by Quental *et al*., suggests that as hypercarnivore species age, they become progressively more "crowded" in the eco-morpho-space. This increase in crowding is interpreted as an increase in competition pressure as species age, which could represent an ecological mechanism for an increase in extinct risk as species become older. To some extent, this is similar to the "evolutionary stasis hypothesis" discussed by Cid (2023) which states that under a scenario of morpho-ecological stasis (reviewed and discussed by Eldredge *et al*., 2005), species' long-term stability (e.g., the pattern expected under a model of punctuated equilibrium) might lead to a competitive disadvantage of older species when compared to younger species. This idea also resonates with the work of Pearson (1995) who suggests that factors extrinsic to the species itself might play a very important role in determining positive ADE. Hence, we advocate that an ecological look, as done here by comparing the ADE signal of ecological and phylogenetic species pool, might be a fruitful way forward to properly understand the underlying mechanisms of age-dependent extinction in other lineages.

CONCLUSIONS

1. In this study, we explore the "Law of Constant Extinction" within a well-defined ecological adaptive zone. Our specific objective was to test the hypothesis that distinct species pools, categorized by either phylogeny or ecology, manifest distinct patterns of age-dependent extinction, and thus pool selection interferes with our inference of the "Law of Constant Extinction”. When using a phylogenetic pool of species, we observed a diverse range of patterns for Age-Dependent Extinction (ADE). These patterns included both positive ADE - older species being more likely to go extinct (e.g., Hesperocyoninae and Borophaginae) and negative ADE - younger species being more likely to go extinct (e.g., Caninae). However, when we consolidated these subfamilies for a broader family-level analysis, the evidence for ADE was either weak or gave way to strong support for Age-Independent Extinction (AIE).

2. When using an ecological pool of species, we consistently observed positive ADE for hypercarnivores, whereas non-hypercarnivores tended to exhibit a negative ADE. Furthermore, our analysis revealed that phylogenetic species pools with a higher proportion of hypercarnivore species generally displayed positive ADE, while phylogenetic species pools with fewer hypercarnivores tended to show negative ADE.

3. We discuss the observed variability in age-dependency signals across different taxonomic ranks, time windows, and between different species pools. These observations strongly confirm our expectation that the choice of species pool has a substantial influence on the signal of age-dependent extinction, and that ecology has a relevant impact on determining the regime of age-dependent extinction.

RESUMO

De acordo com o trabalho seminal de Van Valen (1973), a extinção ocorre a uma taxa constantemente estocástica dentro de grupos ecologicamente homogêneos ou zonas adaptativas, resultando em uma chance igual de espécies novas e velhas se extinguirem. A Hipótese da Rainha Vermelha foi sugerida como um possível mecanismo para esse padrão de taxas de extinção independentemente da idade, que foi chamada de "A Lei da Extinção Constante". O desafio de definir esses grupos homogêneos é explicitamente discutido no trabalho de Van Valen (1973), o que se relaciona com a dificuldade de identificar o conjunto de espécies pertencentes a uma dada zona adaptativa. Níveis taxonômicos superiores são tipicamente usados como uma aproximação prática para zonas adaptativas, e a maioria dos estudos utilizam conjuntos de espécies definidos pela taxonomia ou filogenia para testar a "Lei da Extinção Constante". No entanto, fica claro que Van Valen ao explorar a interpretação da "Lei da Extinção Constante" e a hipótese da Rainha Vermelha entendia as zonas adaptativas sob a ótica de fatores ecológicos. Nesse sentido, um conjunto de espécies definido pela ecologia estaria mais alinhado com o conceito original de Van Valen de zona adaptativa e sua hipótese da Rainha Vermelha. Usando o registro fóssil da família Canidae e uma abordagem bayesiana, demonstramos que os conjuntos de espécies definidos tanto pela filogenia quanto pela ecologia exibem diferentes dinâmicas de extinção dependentes da idade. Encontramos uma considerável variação no sinal de extinção dependente da idade (ADE), dependendo do conjunto de espécies, da janela de tempo usada e do nível taxonômico. Dentro de conjuntos de espécies definidos pela filogenia, observamos evidências para ADE, com tendências tanto positivas - espécies mais velhas com maior probabilidade de extinção (por exemplo, Hesperocyoninae e Borophaginae) quanto negativas - espécies mais jovens mais propensas a se extinguirem (por exemplo, Caninae). Quando as subfamílias são consolidadas em uma análise a nível de família, encontramos evidências fracas para ADE ou suporte robusto para extinção independente da idade (AIE). Além disso, os hipercarnívoros consistentemente exibiram evidências de extinção dependente da idade positiva, enquanto os não-hipercarnívoros evidências de extinção dependente da idade negativa. Também encontramos que clados com uma proporção maior de espécies hipercarnívoras tendiam a exibir um sinal condizente com um ADE positivo, enquanto clados com menos hipercarnívoros tendiam a apresentar um sinal condizente com um ADE negativo. Essas descobertas enfatizam que a escolha do conjunto de espécies influencia inferência das dinâmicas de extinção dependente da idade e que a ecologia tem um impacto relevante na determinação do regime de extinção dependente da idade.

Palavras-chaves: Extinção dependente de idade, Extinção, Macroevolução, Canidae, Hipótese da Rainha Vermelha.

ABSTRACT

According to Van Valen's seminal work (1973), extinction occurs at a constantly stochastic rate within ecologically homogeneous groups or adaptive zones, resulting in an equal chance of long and short-lived species going extinct. The Red Queen Hypothesis was suggested as a possible mechanism for this age-independent extinction rate, which has been named "The Law of Constant Extinction”. The challenge of defining these homogeneous groups is explicitly discussed in Van Valen's work (1973), which relates to the difficulty of identifying the pool of species belonging to a given adaptive zone. Higher taxa have been used as a practical approximation for such adaptive zones, and most studies have used a taxonomically or phylogenetically defined pool of species to test the "Law of Constant Extinction". However, it becomes clear that Van Valen fundamentally viewed adaptive zones through the lens of ecological factors when delving into the interpretation of the "law of constant extinction" and exploring the Red Queen hypotheses. In that respect, an ecologically defined pool of species would be more in line with Van Valen's original concept of the adaptive zone and his underlying Red Queen hypothesis. Using the Canidae fossil record and a Bayesian framework, we demonstrate that species pools defined either by phylogeny or ecology exhibit different age-dependent extinction dynamics. We find considerable variation in the age-dependent extinction signal (ADE), depending on the species pool choice, time window used, and taxonomic level. Within phylogenetic species pools, we observe mixed evidence for ADE, with both positive – older species being more likely to go extinct (e.g., Hesperocyoninae and Borophaginae) and negative - younger species being more likely to go extinct (e.g., Caninae) trends. When subfamilies are consolidated into a single family-level analysis, we encounter either weak evidence for ADE or robust support for Age-independent extinction (AIE). Furthermore, within ecologically defined species pools, hypercarnivores consistently display strong evidence for positive age-dependent extinction, whereas non-hypercarnivores have strong evidence for negative age-dependent extinction. We also found that clades with a higher proportion of hypercarnivore species tended to display evidence for positive age-dependent extinction, while clades with fewer hypercarnivores tended to evidence for negative age-dependent extinction. These findings collectively emphasize that the choice of species pool significantly influences the observed age-dependent extinction dynamics, and that ecology has a relevant impact on determining the regime of age-dependent extinction.

Keywords: Age-independent Extinction, Extinction, Macroevolution, Canidae, Red Queen Hypothesis.

REFERENCES

Balisi, M., Casey, C., Van Valkenburgh, B. (2018). Dietary specialization is linked to reduced species durations in North American fossil canids. *Royal Society Open Science* 5:171861.

Balisi, M., Van Valkenburgh, B. (2020). Iterative evolution of large-bodied hypercarnivory in canids benefits species but not clades. *Communications Biology*, 3:461.

Balmford, A. (1996). Extinction filters and current resilience: The significance of past selection pressures for conservation biology. *Trends in Ecology & Evolution,* 11(5):193–196.

Bambach, R. K. (2006). Phanerozoic biodiversity mass extinctions. *Annual Review of Earth Planetary Sciences* 34:127–155.

Barnosky, A. D. (2001). Distinguishing the effects of the Red Queen and Court Jester on Miocene mammal evolution in the northern Rocky Mountains. *Journal of Vertebrate Paleontology* 21:172–185.

Bengtson, P. (1988). Open nomenclature. *Paleontology* 31:223–227.

Benton, M. J. (2009). The Red Queen and the Court Jester: species diversity and the role of biotic and abiotic factors through time. *Science* 323:728–732.

Blomberg, S. P., Garland, T., Ives, A. R. (2003). Testing for phylogenetic signal in comparative data: behavioral traits are more labile. *Evolution*, 57(4):717-745.

Brown, J. H, Maurer, B. A. (1986). Body size, ecological dominance, and Cope's rule. *Nature* 324:248–50.

Carbone, C., Teacher, A., Rowcliffe, J. M. (2007). The costs of carnivory. *PLoS Biology* 5:363–368.

Carlos Calderón del Cid (2023). Evolutionary age and extinction probability. PhD thesis at Universidade Federal de Bahia (UFBA)

Chichorro, F., Juslén, A., Cardoso, P. (2019). A review of the relation between species traits and extinction risk. *Biological Conservation* 237:220–229.

Condamine, F. L., Rolland, J., Morlon, H. (2013). Macroevolutionary perspectives to environmental change. *Ecology Letters* 16:72–85.

Condamine, F. L., Romieu, J., Guinot, G. (2019). Climate cooling and clade competition likely drove the decline of lamniform sharks. *Proceedings of the National Academy of Sciences* 116:20584–20590.

Condamine, F. L., Silvestro, D., Koppelhus, E. B., Antonelli, A. (2020). The rise of angiosperms pushed conifers to decline during global cooling. *Proceedings of the National Academy of Sciences* 117:28867–28875.

Condamine, F.L., Guinot, G., Benton, M.J., Currie, P. J. (2021). Dinosaur biodiversity declined well before the asteroid impact, influenced by ecological and environmental pressures. *Nature Communications* 12: 3833.

Crampton, J. S., Cooper, R. A., Sadler, P. M., Foote, M. (2016). Greenhouse ice–house transition in the Late Ordovician marks a step-change in extinction regime in the marine plankton. *Proceedings of the National Academy of Sciences* 113:1498– 1503.

Damuth, J. (1981). Population density and body size in mammals. *Nature* 290:699–700.

Damuth, J. (1987). Interspecific allometry of population density in mammals and other animals: the independence of body mass and population energy–use. *Biological Journal of the Linnean Society* 31:193–246.

Debastiani, V. J., Bastazini, V. A., & Pillar, V. D. (2021). Using phylogenetic information to impute missing functional trait values in ecological databases. *Ecological Informatics*, 63:101315.

Delignette-Muller, M.L. and Dutang, C. (2015). Fitdistrplus: An R Package for Fitting Distributions. Journal of Statistical Software, 64, 1-34

Doran, N. A., Arnold, A. J., Parker, W. C., Huffer, F. W. (2006). Is extinction age-dependent? *Palaios* 21:571–579.

Eldredge N., Thompson J.N., Brakefield P.M., Gavrilets S., Jablonski D., Jackson J.B.C., Lenski R.E., Lieberman B.S., McPeek M.A., and Miller W. (2005). The dynamics of evolutionary stasis. *Paleobiology* 31(2):133–145.

Ezard, T. H. G., Aze, T., Pearson, P. N., Purvis, A. (2011). Interplay between changing climate and species' ecology drives macroevolutionary dynamics. *Science* 332:349–351.

Ezard, T. H. G., Quental, T. B., Benton, M. J. (2016). The challenges to inferring the regulators of biodiversity in deep time. *Philosophical Transactions of the Royal Society B: Biological Sciences* 371:20150216.

Faurby, S., Werdelin, L. & Antonelli, A. (2019). Dispersal ability predicts evolutionary success among mammalian carnivores. *BioXRiv*.

Faurby, S., Morlo M., & Werdelin L. (2021). CarniFOSS: A database of the body mass of fossil carnivores. *Global Ecology and Biogeography* 00:1–7.

Finnegan, S., Payne, J. L., Wang, S. C. (2008). The Red Queen revisited: reevaluating the age selectivity of Phanerozoic marine genus extinctions. *Paleobiology* 34:318–341.

Foote, M., Crampton, J. S., Beu, A. G., Cooper, R. A. (2008). On the bidirectional relationship between geographic range and taxonomic duration. *Paleobiology* 34:421–433.

Foote, M., Raup, D. M. (1996). Fossil preservation and the stratigraphic ranges of taxa. Paleobiology 22:121–140.

Goolsby, E. W., Bruggeman, J., & Ané, C. (2016). Rphylopars: Fast multivariate phylogenetic comparative methods for missing data and within-species variation. *Methods in Ecology and Evolution* 8:22–27.

Griffiths, D. (1980). Foraging Costs and Relative Prey Size. *The American Naturalist* 116(5):743–752.

Hagen, O., Andermann, T., Quental, T. B., Antonelli, A., Silvestro, D. (2018). Estimating age-dependent extinction: contrasting evidence from fossils and phylogenies. *Systematic Biology* 67:458–474.

Hembry, D. H., and M. G. Weber. (2020). Ecological interactions and macroevolution: A new field with old roots. *Annual Review of Ecology Evolution and Systematics* 51:215–243.

Hillebrand, H. (2004). On the Generality of the Latitudinal Diversity Gradient. *The American Naturalist.*

Hoekstra, H. & Fagan, W. (1998). Body size, dispersal ability and compositional disharmony: The carnivore-dominated fauna of the Kuril Islands. *Diversity and Distributions* 4(3):135-149.

Holliday, J. A., Steppan, S. J. (2004). Evolution of hypercarnivory: the effect of specialization on morphological and taxonomic diversity. *Paleobiology* 30:108–128.

Hopkins, S., Price, S., Chiono, A. (2021). Influence of phylogeny on the estimation of diet from dental morphology in the Carnivora. *Paleobiology* 48(2):324-339.

Jablonski D. (2008) Biotic interactions and macroevolution: extensions and mismatches across scales and levels. *Evolution* 62:715–739.

Janis, C. M., Scott, K. M., Jacobs, L. L. (1998). Evolution of Tertiary Mammals of North America: Volume 1, Terrestrial Carnivores, Ungulates, and Ungulate Like Mammals

Januario, M., Quental T.B. (2021). Re-evaluation of the “law of constant extinction” for ruminants at different taxonomical scales. *Evolution* 3:656–671.

Johnson, T. F., B. Isaac, N. J., Paviolo, A., González-Suárez, M. (2021). Handling missing values in trait data. *Global Ecology and Biogeography* 30(1):51-62

Jones, D. S., Nicol, D. (1986). Origination, survivorship, and extinction of rudist taxa. *Journal of Paleontology* 60:107–115.

Jouault, C., Nel, A., Perrichot, V., Legendre, F., & Condamine, F. L. (2022). Multiple drivers and lineage-specific insect extinctions during the Permo–Triassic. *Nature Communications* 13(1):1-16.

Kass, R. E., Raftery, A. E. (1995). Bayes Factors. *Journal of the American Statistical Association* 90:773–795.

Kirschner, M. & Gerhart J. (1998). Evolvability. *Proceedings of the National Academy of Sciences of the United States of America* 95:8420–8427.

Liow, L. H., and N. C. Stenseth. (2007). The rise and fall of species: Implications for macroevolutionary and macroecological studies. *Proceedings of the Royal Society B: Biological Sciences* 274:2745–2752.

Liow, L. H., Reitan, T., Harnik, P. G. (2015). Ecological interactions on macroevolutionary time scales: clams and brachiopods are more than ships that pass in the night. *Ecology Letters* 18:1030–1039.

Liow, L. H., Van Valen, L., Stenseth, N. C. (2011). Red Queen: from population to taxa and communities. *Trends in Ecology & Evolution* 26:349–358.

McKinney, M. L. (1997). Extinction Vulnerability and Selectivity: Combining Ecological and Paleontological Views. *Annual Review of Ecology and Systematics* 28:495–516.

Miller, A. I. (1997). A new look at age and area: the geographic and environmental expansion of genera during the Ordovician Radiation. *Paleobiology* 23:410–419.

Mittelbach, G. G., Schemske, D. W., Cornell, H. V., Allen, A. P., Brown, J. M., Bush, M. B. *et al*. (2007). Evolution and the latitudinal diversity gradient: speciation, extinction, and biogeography. *Ecology Letters* 10:315–331.

Molina-Venegas, R., Moreno-Saiz, J. C., Castro Parga, I., Davies, T. J., Peres-Neto, P. R., & Rodríguez, M. (2018). Assessing among-lineage variability in phylogenetic imputation of functional trait datasets. *Ecography* 41:1740–1749.

Muller, H. J. (1964). The relation of recombination to mutational advance. *Mutation Research/ Fundamental and Molecular Mechanisms of Mutagenesis* 1:2–9.

Pagel, M. (1999). Inferring the historical patterns of biological evolution. *Nature* 401(6756):877-884.

Paradis, E., Claude, J. & Strimmer, K. (2004). APE: Analyses of Phylogenetics and Evolution in R language. *Bioinformatics* 20(2): 289-290.

Parker, W. C., Arnold, A. J. (1997). Species survivorship in the Cenozoic planktonic foraminifera: A test of exponential and Weibull models. *Palaios* 12:3–11.

Payne, J. L., Finnegan, S. (2007). The effect of geographic range on extinction risk during background and mass extinction. *Proceedings of the National Academy of Sciences* 104:10506–10511.

Pearson, P. N. (1995). Investigating age–dependency of species extinction rates using dynamic survivorship analysis. *Historical Biology* 10:119–136.

Penone, C., Davidson, A. D., Shoemaker, K. T., Di Marco, M., Rondinini, C., Brooks, T. M., Costa, G. C. (2014). Imputation of missing data in life-history trait datasets: Which approach performs the best? *Methods in Ecology and Evolution* 5:961–970.

Pires, M. M., Silvestro, D., Quental, T. B. (2015). Continental faunal exchange and the asymmetrical radiation of carnivores. *Proceedings of the Royal Society B* 282:20151952.

Pires, M. M., Silvestro, D., Quental, T. B. (2017). Interactions within and between clades shaped the diversification of terrestrial carnivores. *Evolution* 71:1855–1864.

Purvis, A., Gittleman, J. L., Cowlishaw, G., Mace, G. M., (2000). Predicting extinction risk in declining species. *Proceedings of the Royal Society B: Biological Science* 267:1947–1952.

Rambaut, A., Drummond, A. J., Xie, D., Baele, G., Suchard, M. A. (2018). Posterior Summarization in Bayesian Phylogenetics Using Tracer 1.7. *Systematic Biology* 67(5):901-904.

Rasmussen, G. S. A., Gusset, M., Courchamp, F., Macdonald, D. W. (2008). Achilles' heel of sociality revealed by energetic poverty trap in cursorial hunters. *The American Naturalist* 172:508–518.

Raup D. M., Sepkoski J.J. (1982). Mass extinctions in the marine fossil record. *Science* 215:1501–1503.

Raup, D. M. (1985). Mathematical models of cladogenesis. *Paleobiology* 11:42–52

Revell, L.J. (2012). phytools: An R package for phylogenetic comparative biology (and other things). *Methods in Ecology and Evolution* 3(2):217–223.

Robert E. Kass & Adrian E. Raftery. (1995). Bayes Factors, *Journal of the American Statistical* Association 90(430):773-795.

Rosenblum, E. B., Sarver, B. A. J., Brown, J. W., Des Roches, S., Hardwick, K. M., Hether, T. D., Eastman, J. M., Pennell, M. W., Harmon, L. J. (2012). Goldilocks Meets Santa Rosalia: An Ephemeral Speciation Model Explains Patterns of Diversification Across Time Scales. *Evolutionary Biology* 39:255–261.

Saulsbury, J. G., Parins-Fukuchi, C. T., Wilson, C. J., Reitan, T., Liow, L. H. (2023) Age-dependent extinction and the neutral theory of biodiversity. *BioXRiv.*

Schlaepfer, M. A., Runge, M. C., Sherman, P. W. (2002). Ecological and evolutionary traps. *Trends in Ecology & Evolution* 17:474–480.

Sigovini, M., Keppel, E., Tagliapietra, D. (2016). Open Nomenclature in the biodiversity era. *Methods in Ecology and Evolution* 7:1217–1225.

Silvestro, D., Antonelli, A., Salamin, N., Quental, T. B. (2015). the role of clade competition in the diversification of North American canids. *Proceedings of the National Academy of Sciences* 112:8684–8689.

Silvestro, D., Castiglione, S., Mondanaro, A., Serio, C., Melchionna, M., Piras, P., Di Febbraro, M., Carotenuto, F., Rook, L., Raia, P. (2020). A 450 million yearlong latitudinal gradient in age–dependent extinction. *Ecology Letters* 23:439–446.

Silvestro, D., Salamin, N., Antonelli, A., Meyer, X. (2019). Improved estimation of macroevolutionary rates from fossil data using a Bayesian framework. *Paleobiology* 45:546–570.

Silvestro, D., Salamin, N., Schnitzler, J. (2014). PyRate: A new program to estimate speciation and extinction rates from incomplete fossil data. *Methods in Ecology and Evolution* 5:1126–1131.

Simpson, G. G. (1944). *Tempo and mode in evolution*. Columbia University Press, New York.

Simpson, G. G. (1953). *The major features of evolution*. New York: Columbia University. Press

Slater, G. J. (2015). Iterative adaptive radiations of fossil canids show no evidence for diversity–dependent trait evolution. *Proceedings of the National Academy of Sciences* 112:4897–4902.

Smits, P. D. (2015). Expected time-invariant effects of biological traits on mammal species duration. *Proceedings of the National Academy of Sciences* 112(42):13015–13020

Sorkin, B. (2008). A biomechanical constraint on body mass in terrestrial mammalian predators. *Lethaia* 41:333–347.

Stanley, S. M. (1979). *Macroevolution*. San Francisco: Freeman.

Stanley, S. M. (1979). *Macroevolution: Patterns and Process*. Freeman.

Stenseth, N. C., Maynard Smith, J. (1984). Coevolution in ecosystems – Red Queen evolution or stasis. *Evolution* 38:870–880.

Tedford, R. H., Wang, X., Taylor, B. E. (2009) Phylogenetic Systematics of the North American Fossil Caninae (Carnivora: Canidae). *Bulletin of the American Museum of Natural History* 325:1–218.

Van Valen, L. (1971). Adaptive zones and the orders of mammals. *Evolution* 25(2):420-428.

Van Valen, L. (1973). A new evolutionary law. *Evolutionary Theory* 1:1–30.

Van Valkenburgh, B. (1991). Iterative evolution of hypercarnivory in canids (Mammalia: Carnivora): evolutionary interactions among sympatric predators. *Paleobiology* 17:340–362.

Van Valkenburgh, B. (1999). Major patterns in the history of carnivorous mammals. *Annual Review of Earth and Planetary Science* 27:463–493.

Van Valkenburgh, B. (2007). Déjà vu: The evolution of feeding morphologies in the Carnivora. *Integrative and Comparative Biology* 47(1):147–163

Van Valkenburgh, B., & K.-P. Koepfli. (1993). Cranial and dental adaptations to predation in canids. *Symposia of the Zoological Society of London* 65:15–37.

Van Valkenburgh, B., Wang, X. & Damuth, J (2004). Cope's rule, hypercarnivory, and extinction in North American canids. *Science* 306:101–104.

Venables, W.N. & Ripley, B.D. (2002). *Modern Applied Statistics with S* (Springer, New York), 4th Ed.

Vermeij, G. J. (1973). Biological Versatility and Earth History. *Proceedings of the National Academy of Sciences of the United States of America,* 70(7):1936-1938.

Viranta, S. (2003). Geographic and temporal ranges of Middle and Late Miocene carnivores. *Journal of Mammalogy* 84:1267–1278.

Vrba, E. S. & DeGusta, D. (2004). Do species populations really start small? New perspectives from the Late Neogene fossil record of African mammals. *Philosophical Transactions of the Royal Society B: Biological Sciences* 359:285–92–discussion 292–293.

Wagner, A. (2008). Robustness and evolvability: A paradox resolved. *Proceedings of the Royal Society B: Biological Sciences*, 275(1630):91-100.

Wang, X. (1994). Phylogenetic Systematics of the Hesperocyoninae (Carnivora, Canidae). *Bulletin of the American Museum of Natural History.*

Wang, X., Tedford, R. H. (2008). *Dogs: their fossil relatives and evolutionary history*. Columbia University Press.

Wang, X., Tedford, R. H., Taylor, B. E. (1999). Phylogenetic Systematics of the Borophaginae (Carnivora: Canidae). *Bulletin of the American Museum of Natural History* 243:1–390.

Zeng, Y. & J. J. Wiens. (2021). Species interactions have predictable impacts on diversification. *Ecology Letters* 24.2: 239–248.

Zrzavý, J., Duda, P., Robovský, J., Okřinová, I., Pavelková Řičánková, V. (2018). Phylogeny of the Caninae (Carnivora): Combining morphology, behaviour, genes, and fossils. *Zoologica Scripta* 47:373–389.

SUPPLEMENTARY MATERIAL

Supplementary figures

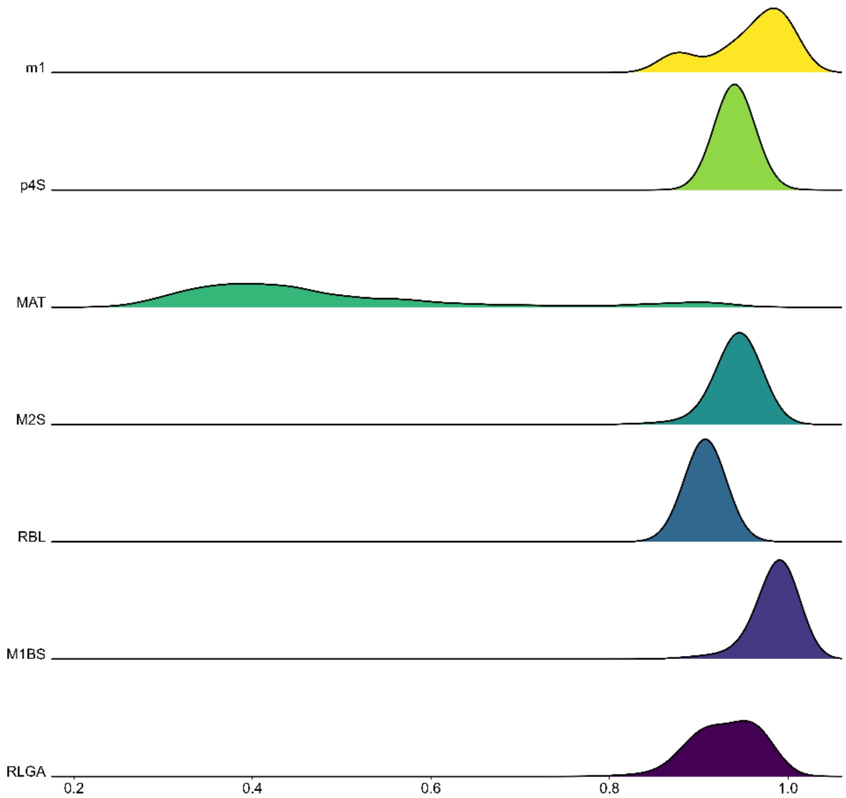

Figure S1. Estimates of Pagel's lambda for the seven craniodental variables (m1, p4S, MAT, M2S, RBL, M1BS, and RLGA) using the 1000 trees provided by Faurby *et al*. (2019).

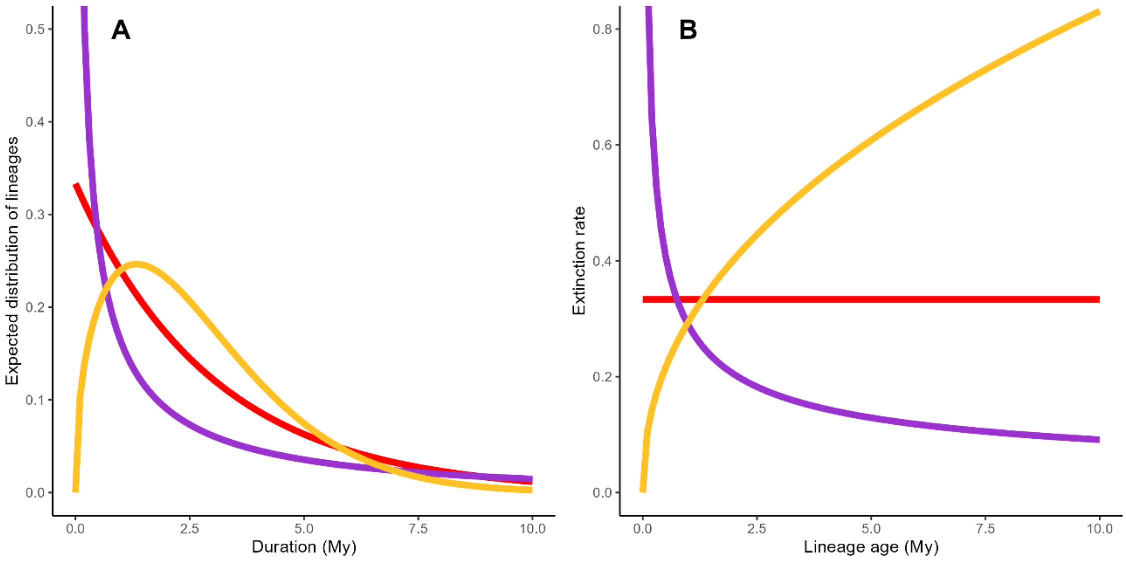

Figure S2. Expectations for the distribution of lineage durations (panel A) and extinction rate as a function of age (panel B), using the Weibull model from Hagen *et al*, 2018. When lineages are under negative age-dependent extinction, the shape parameter of the predicted distribution of lineage duration is less than one (panel A, purple line), and the extinction rate is greater for young lineages but decreases as the lineage ages (panel B, purple line). When there is positive age-dependent extinction of lineages, the shape parameter of the predicted distribution of lineage duration is greater than 1 (panel A, yellow line), and the extinction rate is lower for younger lineages and increases as the lineage gets older (panel B, yellow line). When lineages exhibit age-independent extinction, the shape parameter of the predicted distribution of lineage durations approaches 1 (panel A, red line), and the extinction remains constant across different lineage ages (panel B, red line).

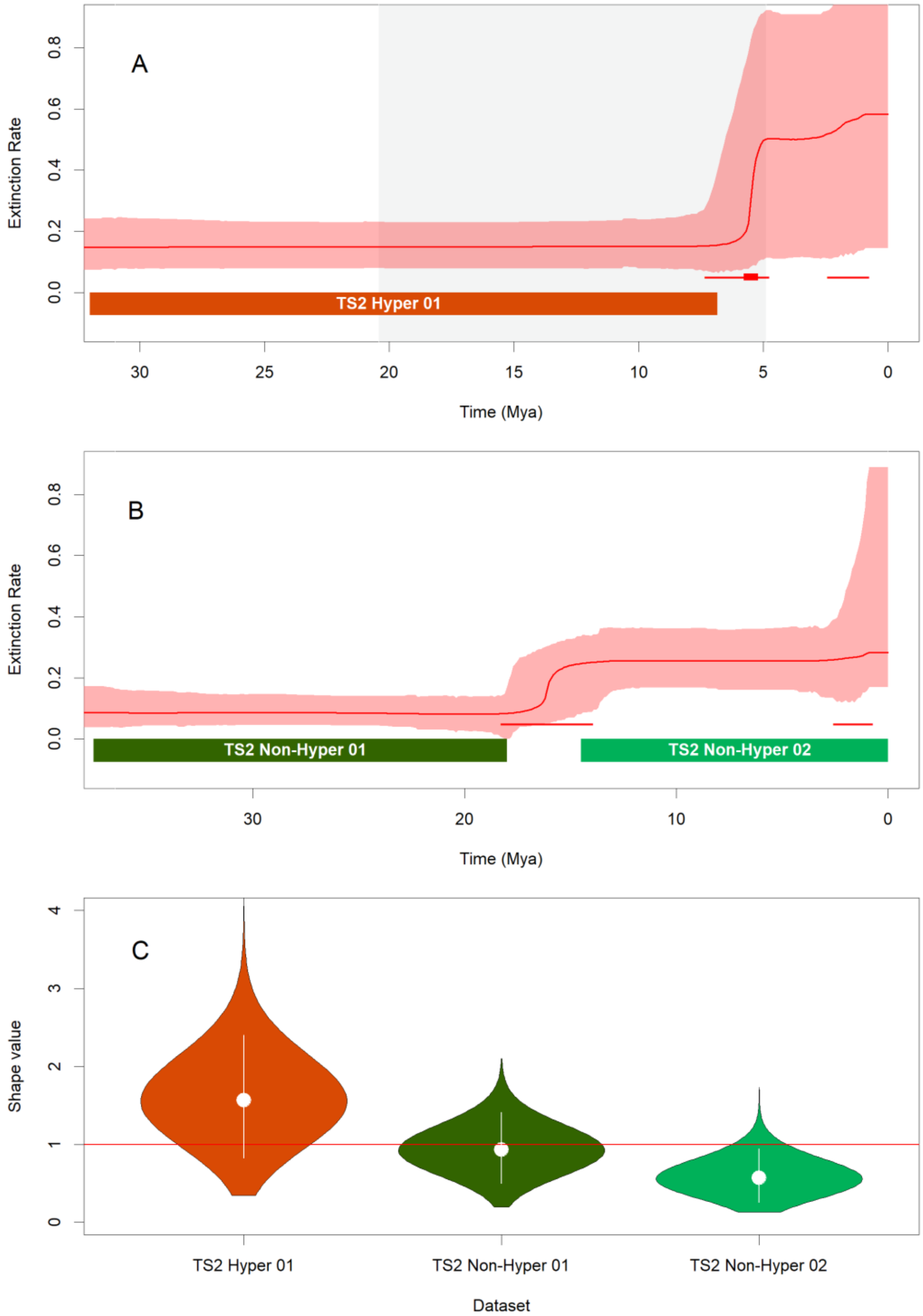

Figure S3. Extinction rate and age-dependency in hypercarnivores and non-hypercarnivores for the second training set (TS2). Panels A and B display plots of extinction rates over time, with the light-colored area representing the 95% highest posterior density interval (HPD) for the extinction rate of hypercarnivores (panel A) and non-hypercarnivores (panel B). The solid line within the light-colored area represents the median of the posterior distribution of rate values at each time point. Red horizontal segments indicate times of low significance (2 < BF < 6) rate shifts in extinction, while red rectangles mark times of highly significant (BF > 6) rate shifts in speciation and extinction. In panel A, the white and grey background bars indicate the preservation intervals used in the analysis, allowing preservation to vary among but remain constant within intervals. Colored horizontal bars indicate the length of the different time windows used in each ADE analysis. Panel C presents violin plots, combining the posterior distribution for the shape parameter of the Weibull distribution for each time window. The vertical white lines in panel C represent the 95% HPD, and the white dot indicates the median of each posterior distribution. The red horizontal line indicates age-independency (shape value = 1).

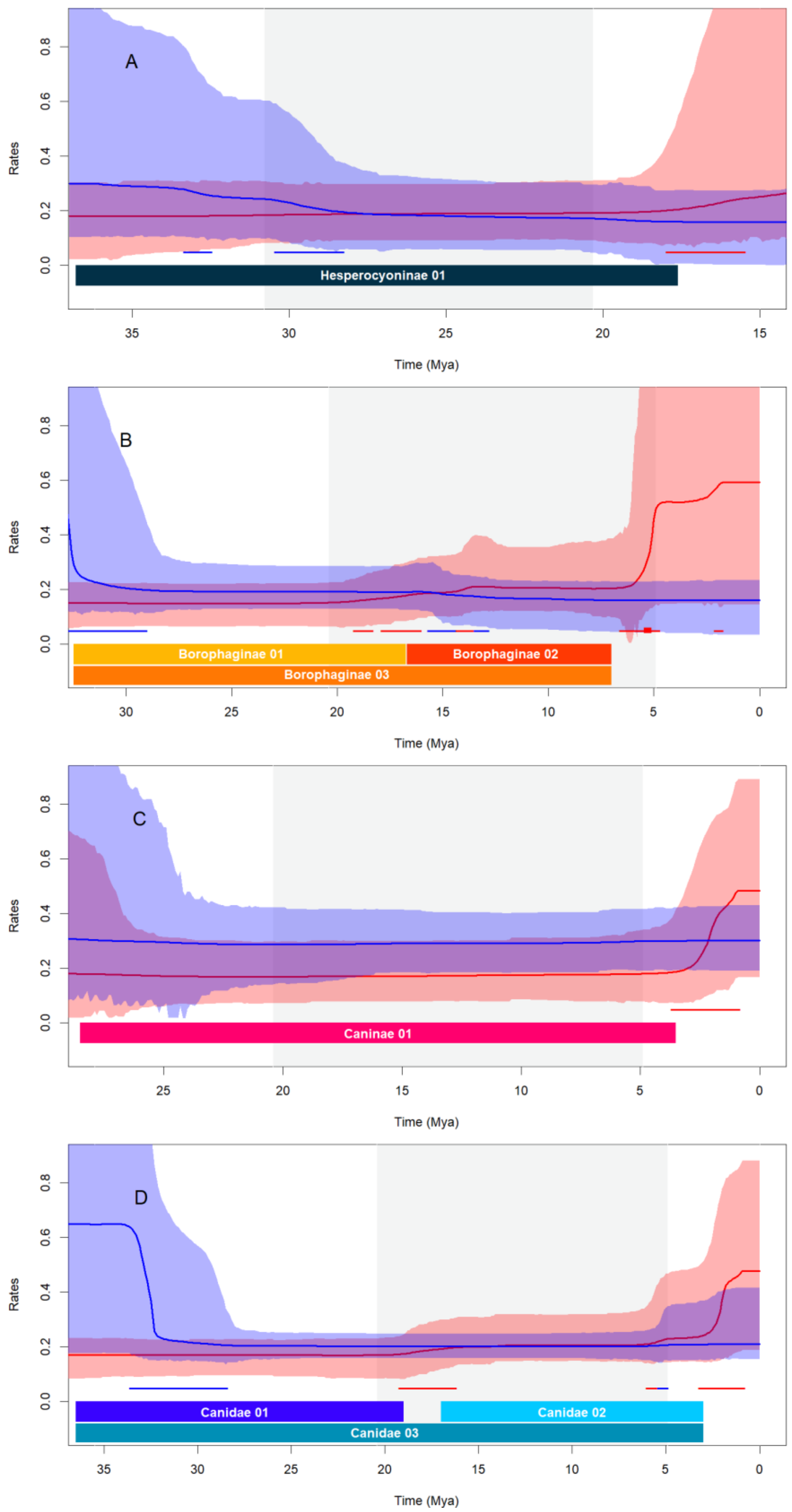

Figure S4. Diversification rate through time (RTT) for Canidae and its subfamilies. Panels A, B, C, and D show RTT plots, with the light-colored area representing the 95% highest posterior density interval (HPD) for the speciation (blue) and extinction (red) rates for Hesperocyoninae (Panel A), Borophaginae (Panel B), Caninae (Panel C), and Canidae (Panel D). The continuous line inside the light-colored area indicates the median of the posterior distribution of rate values at each moment in time. Blue and red horizontal segments indicate times of low significance (2 < BF < 6) rate shifts in speciation and extinction rates, while blue and red rectangles represent the times of highly significant (BF > 6) rate shifts in speciation and extinction. The white and grey background bars indicate the preservation intervals used in the analysis where we allowed preservation to vary among but be constant within intervals (preservation variation among lineages was allowed within each time window). The horizontal-colored bars on the bottom of panels (A), (B), (C), and (D), indicate the length of the different time windows used in each ADE analysis.

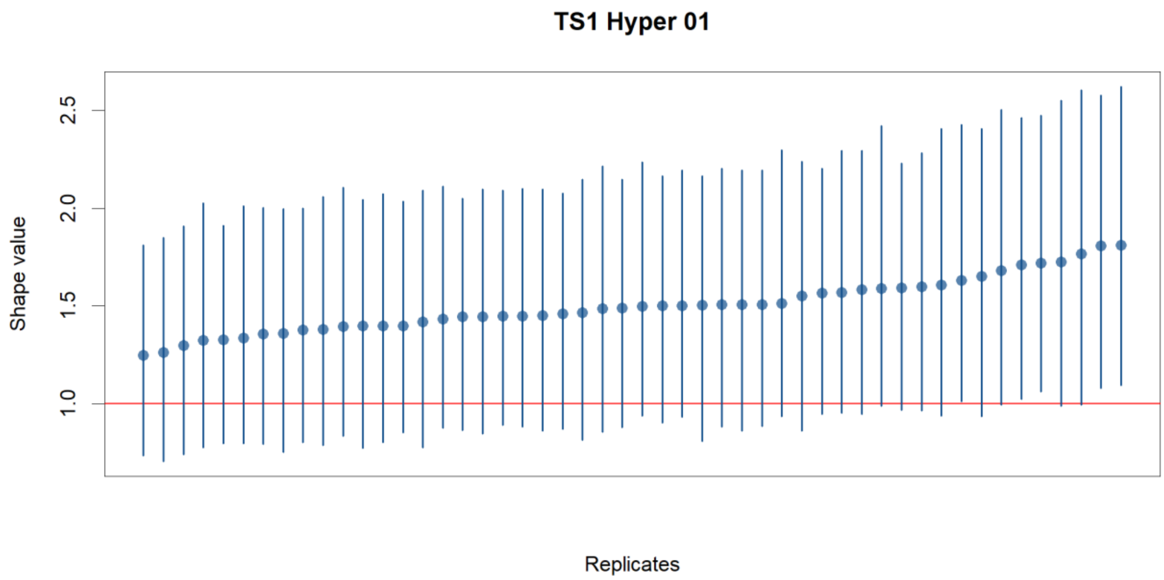

Fig. S5. 95% highest posterior density intervals (HPD) for shape estimates for each replicate in the TS1 Hyper 01 window. The replicates are arranged in order of their median values. The red line represents age-independency, indicated by a shape value of 1.

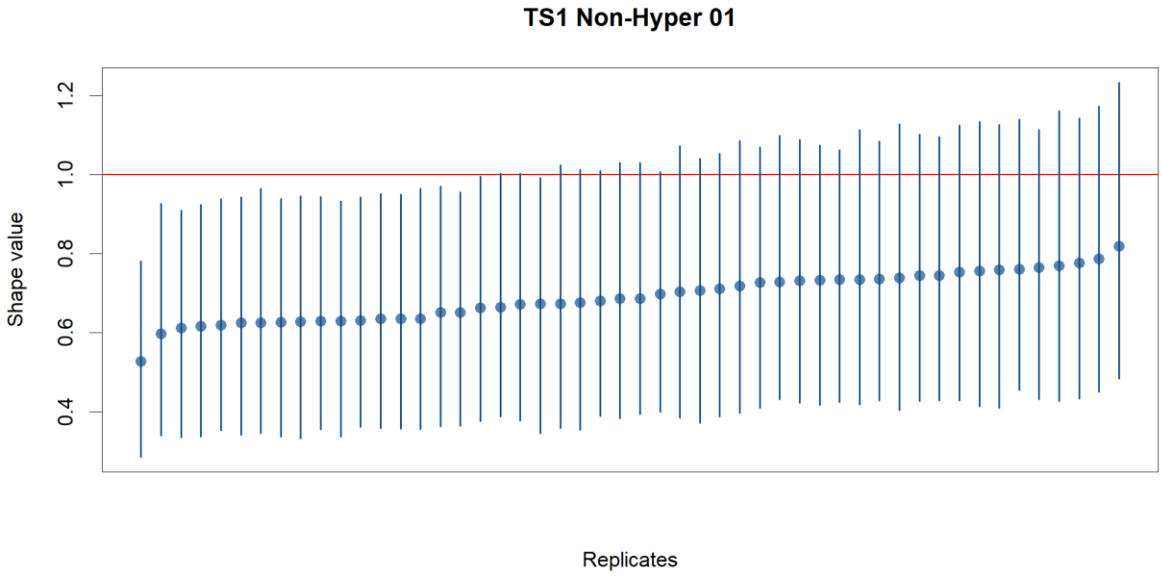

Fig. S6. 95% highest posterior density intervals (HPD) for shape estimates for each replicate in the TS1 Non-Hyper 01 window. The replicates are arranged in order of their median values. The red line represents age-independency, indicated by a shape value of 1.

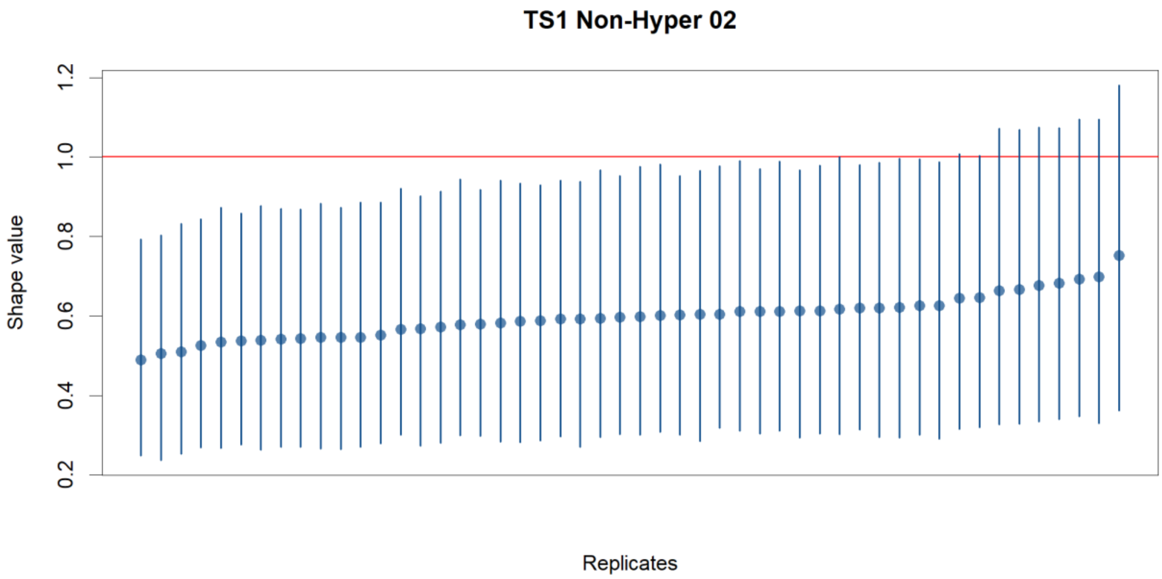

Fig. S7. 95% highest posterior density intervals (HPD) for shape estimates for each replicate in the TS1 Non-Hyper 02 window. The replicates are arranged in order of their median values. The red line represents age-independency, indicated by a shape value of 1.

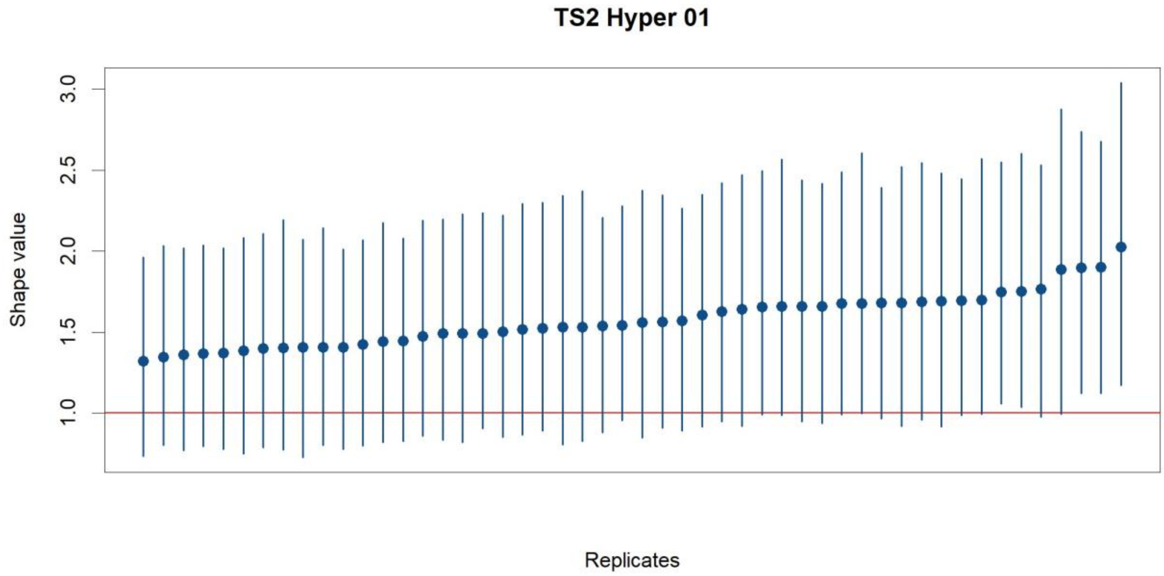

Fig. S8. 95% highest posterior density intervals (HPD) for shape estimates for each replicate in the TS2 Hyper 01 window. The replicates are arranged in order of their median values. The red line represents age-independency, indicated by a shape value of 1.

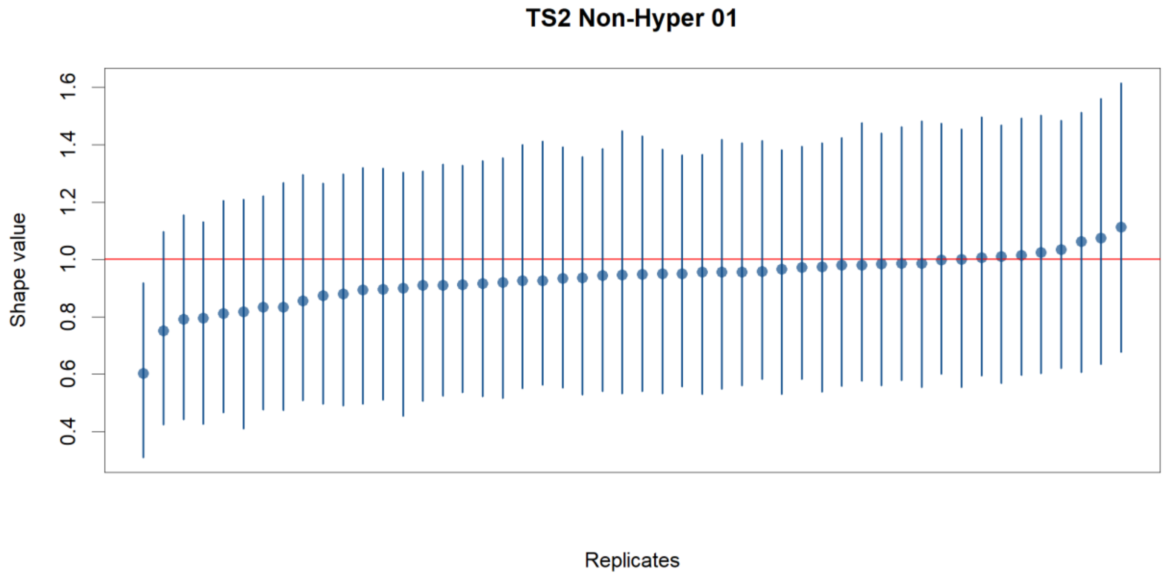

Fig. S9. 95% highest posterior density intervals (HPD) for shape estimates for each replicate in the TS2 Non-Hyper 01 window. The replicates are arranged in order of their median values. The red line represents age-independency, indicated by a shape value of 1.

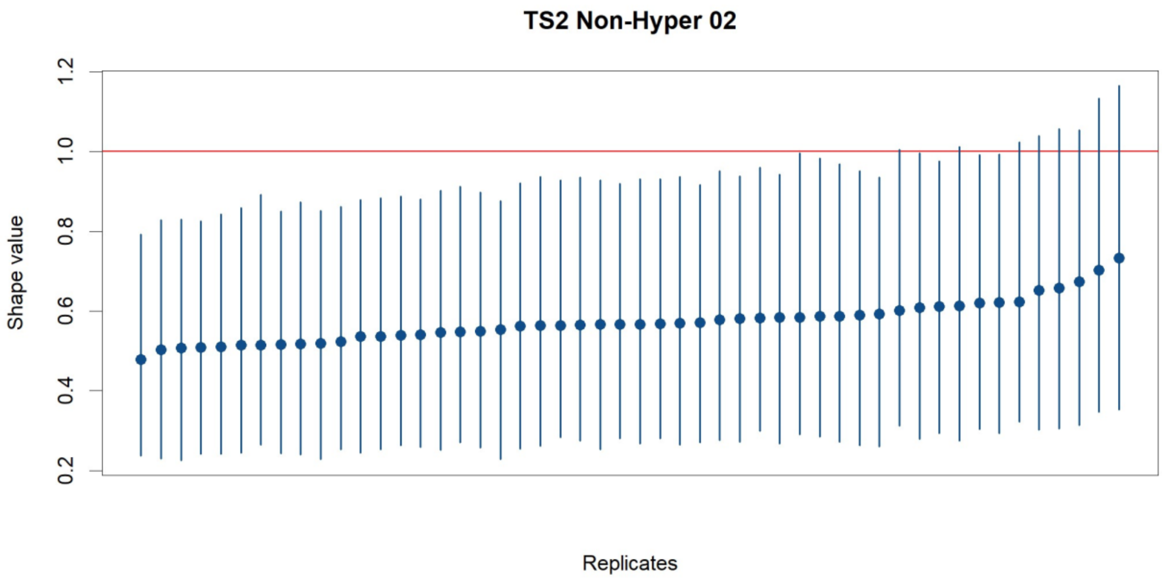

Fig. S10. 95% highest posterior density intervals (HPD) for shape estimates for each replicate in the TS2 Non-Hyper 02 window. The replicates are arranged in order of their median values. The red line represents age-independency, indicated by a shape value of 1.

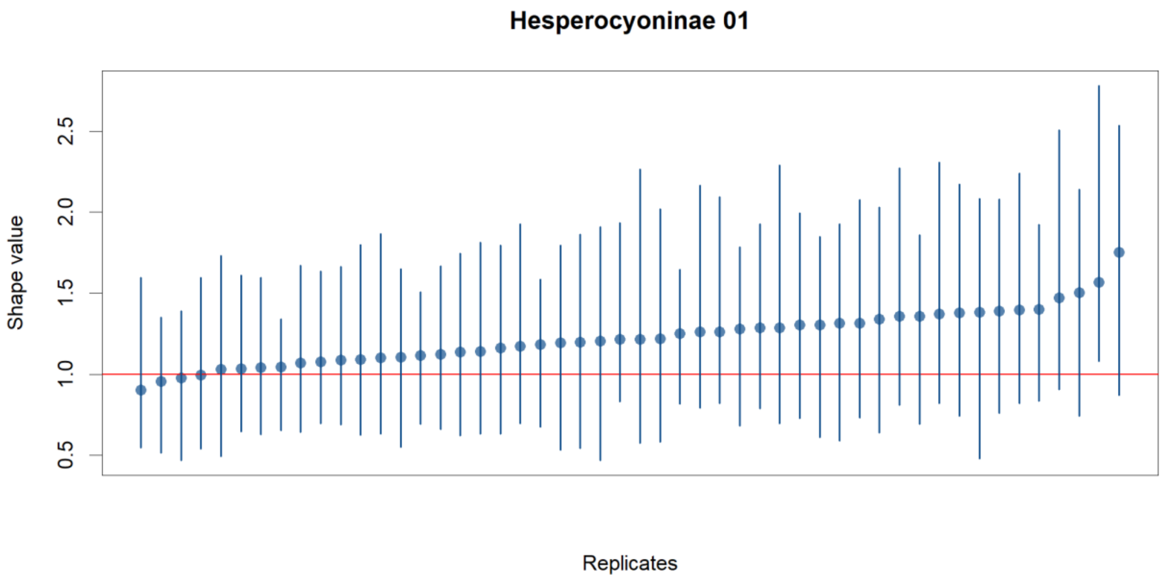

Fig. S11. 95% highest posterior density intervals (HPD) for shape estimates for each replicate in the Hesperocyoninae 01 window. The replicates are arranged in order of their median values. The red line represents age-independency, indicated by a shape value of 1.

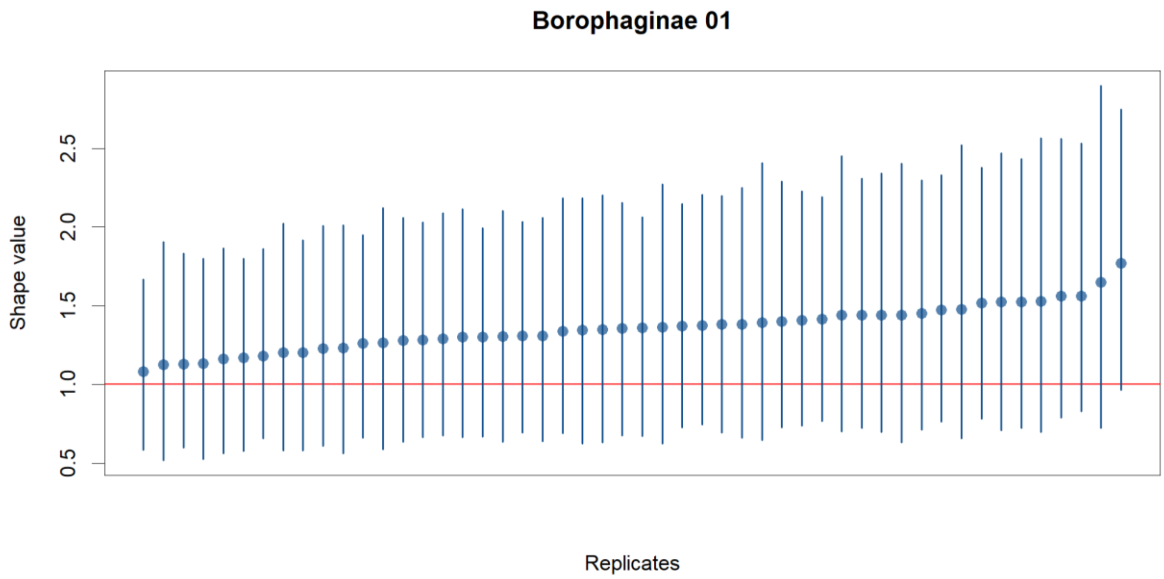

Fig. S12. 95% highest posterior density intervals (HPD) for shape estimates for each replicate in the Borophaginae 01 window. The replicates are arranged in order of their median values. The red line represents age-independency, indicated by a shape value of 1.

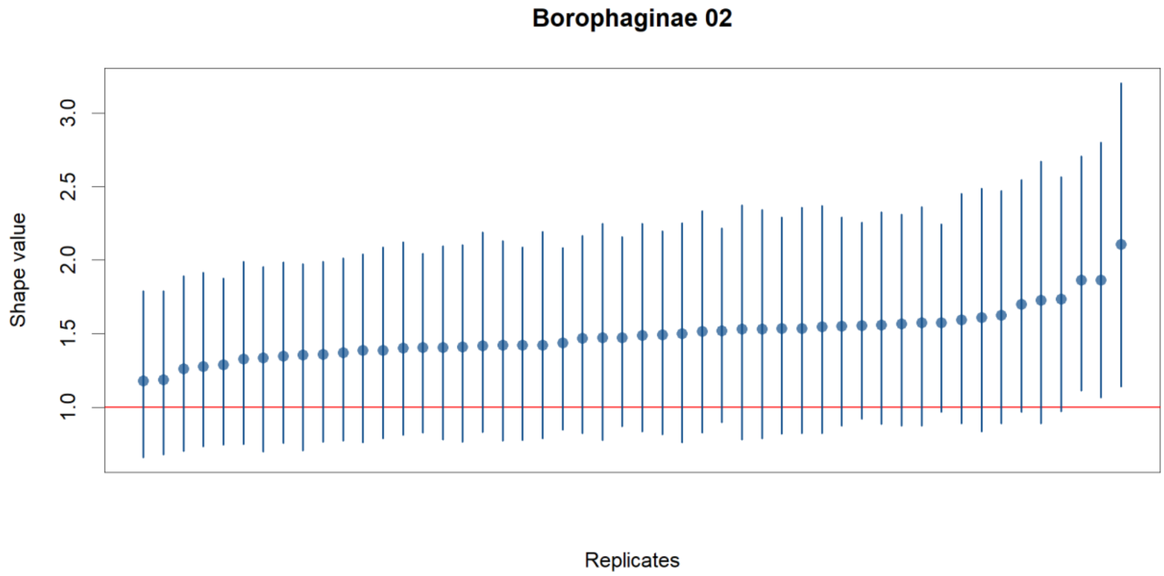

Fig. S13. 95% highest posterior density intervals (HPD) for shape estimates for each replicate in the Borophaginae 02 window. The replicates are arranged in order of their median values. The red line represents age-independency, indicated by a shape value of 1.

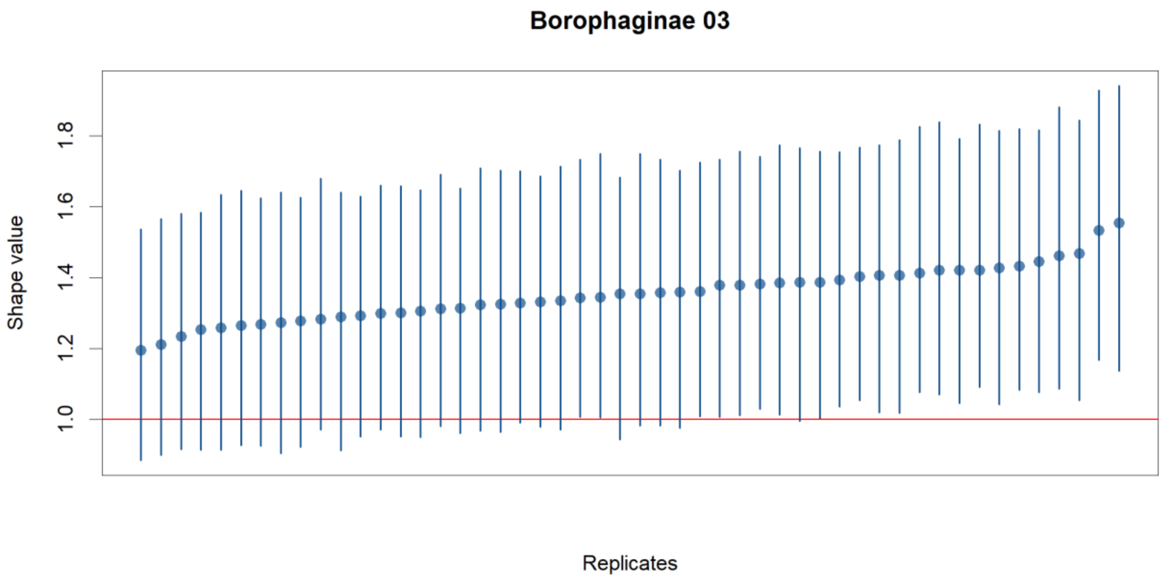

Fig. S14. 95% highest posterior density intervals (HPD) for shape estimates for each replicate in the Borophaginae 03 window. The replicates are arranged in order of their median values. The red line represents age-independency, indicated by a shape value of 1.

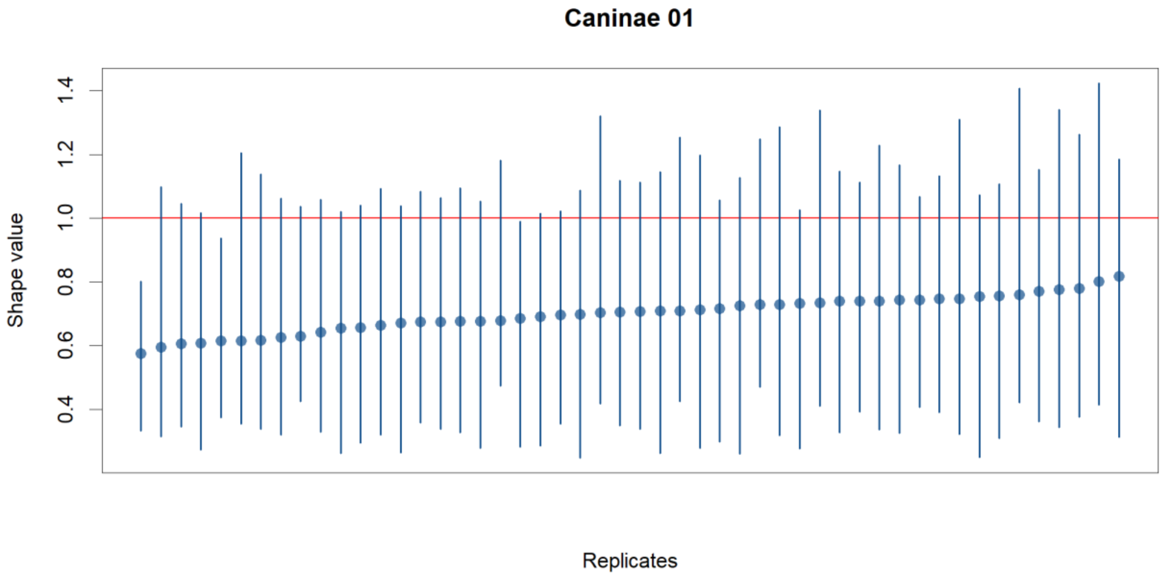

Fig. S15. 95% highest posterior density intervals (HPD) for shape estimates for each replicate in the Caninae 01 window. The replicates are arranged in order of their median values. The red line represents age-independency, indicated by a shape value of 1.

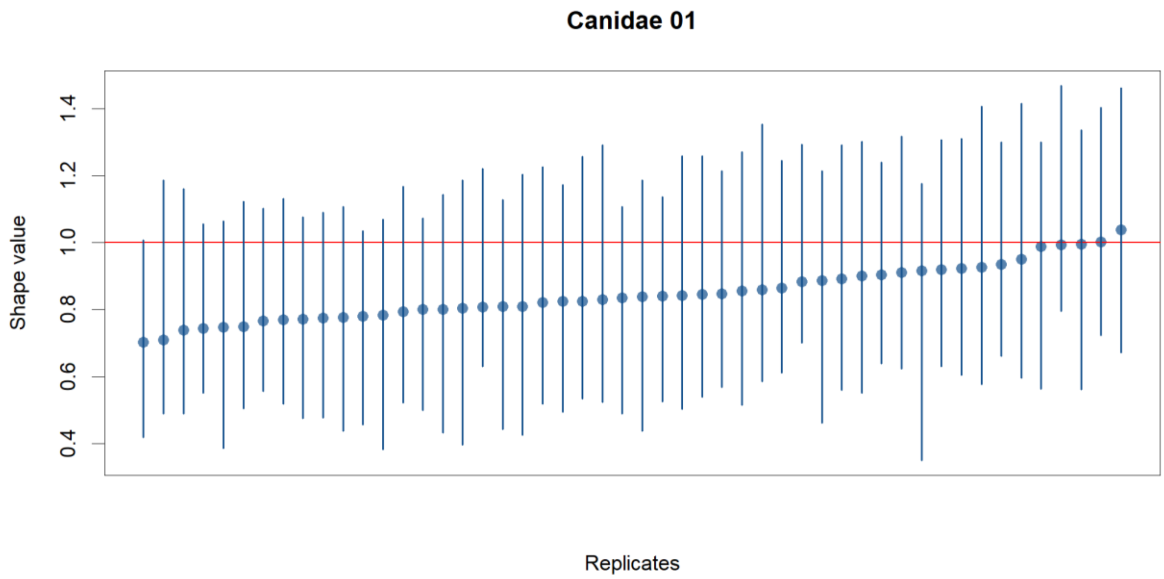

Fig. S16. 95% highest posterior density intervals (HPD) for shape estimates for each replicate in the Canidae 01 window. The replicates are arranged in order of their median values. The red line represents age-independency, indicated by a shape value of 1.

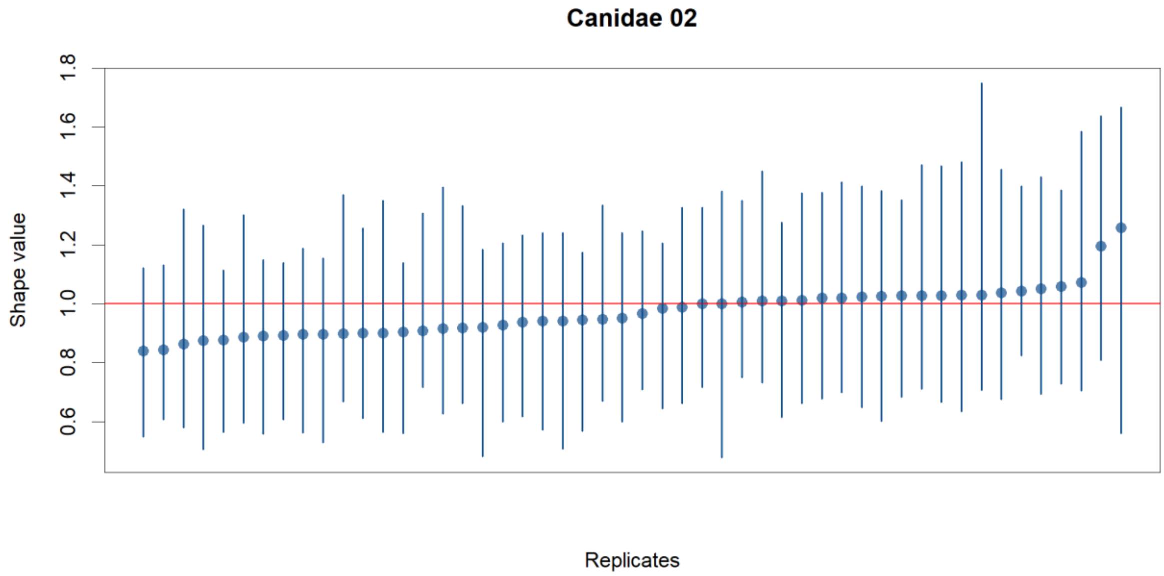

Fig. S17. 95% highest posterior density intervals (HPD) for shape estimates for each replicate in the Canidae 02 window. The replicates are arranged in order of their median values. The red line represents age-independency, indicated by a shape value of 1.

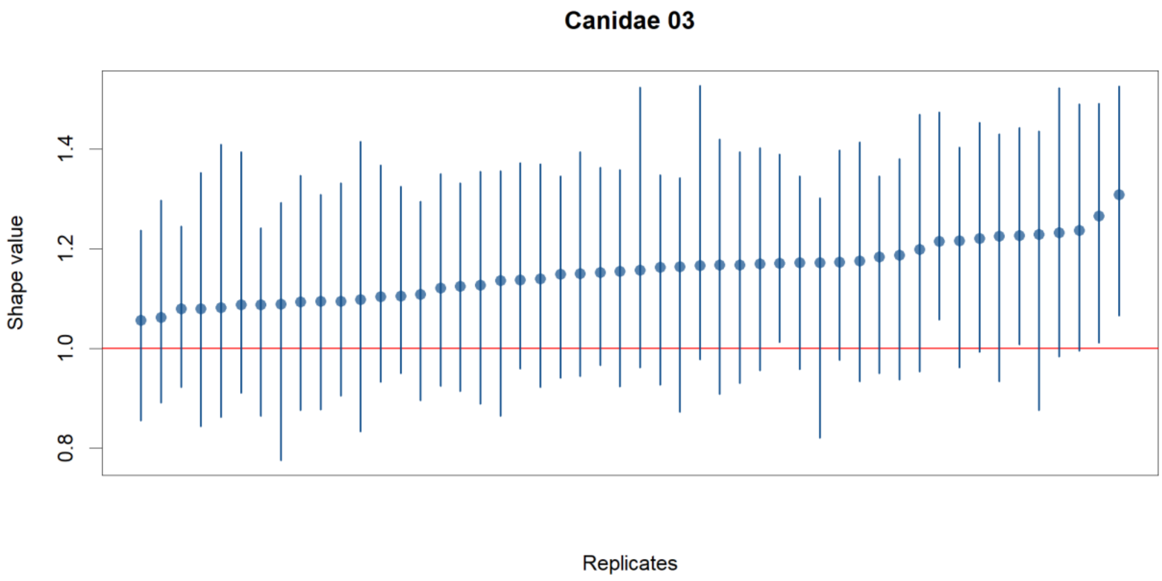

Fig. S18. 95% highest posterior density intervals (HPD) for shape estimates for each replicate in the Canidae 03 window. The replicates are arranged in order of their median values. The red line represents age-independency, indicated by a shape value of 1.

Supplementary table

Supplementary Table 1. Diet Classification of Extant Carnivores in Training Sets. The table presents the diet classification for extant carnivores, divided into two sets: TS1 classification, as proposed by Hopkins *et al*. (2021), and TS2 classification, as proposed by Slater (2015).

Species	TS1	TS2
Ailurus fulgens	Hypocarnivores	Herbivores
Atelocynus microtis	Mesocarnivores	Hypocarnivores
Bassaricyon alleni	Hypocarnivores	Herbivores
Bassaricyon gabbii	Hypocarnivores	Herbivores
Bassariscus astutus	Hypocarnivores	Hypocarnivores
Bassariscus sumichrasti	Hypocarnivores	Hypocarnivores
Canis adustus	Mesocarnivores	Hypocarnivores
Canis aureus	Mesocarnivores	Mesocarnivores
Canis latrans	Mesocarnivores	Mesocarnivores
Canis lupus	Hypercarnivores	Hypercarnivores
Canis mesomelas	Mesocarnivores	Mesocarnivores

Cerdocyon thous	Hypocarnivores	Hypocarnivores
Chrysocyon brachyurus	Mesocarnivores	Hypocarnivores
Cuon alpinus	Hypercarnivores	Hypercarnivores
Lycaon pictus	Hypercarnivores	Hypercarnivores
Nasua narica	Hypocarnivores	Hypocarnivores
Nasua nasua	Hypocarnivores	Hypocarnivores
Nyctereutes procyonoides	Hypocarnivores	Hypocarnivores
Potos flavus	Hypocarnivores	Herbivores
Procyon cancrivorous	Hypocarnivores	Hypocarnivores
Procyon lotor	Hypocarnivores	Hypocarnivores
Pseudalopex culpaeus	Mesocarnivores	Hypocarnivores
Pseudalopex griseus	Mesocarnivores	Hypocarnivores
Pseudalopex gymnocercus	Mesocarnivores	Hypocarnivores
Pseudalopex sechurae	Hypocarnivores	Hypocarnivores
Speothos venaticus	Hypercarnivores	Hypercarnivores
Urocyon cinereoargenteus	Mesocarnivores	Hypocarnivores
Urocyon littoralis	Mesocarnivores	Hypocarnivores
Vulpes bengalensis	Mesocarnivores	Hypocarnivores
Vulpes chama	Mesocarnivores	Hypocarnivores
Vulpes lagopus	Mesocarnivores	Mesocarnivores
Vulpes rueppelli	Mesocarnivores	Hypocarnivores
Vulpes velox	Mesocarnivores	Mesocarnivores
Vulpes vulpes	Mesocarnivores	Mesocarnivores
Vulpes zerda	Hypocarnivores	Hypocarnivores

CODE APPENDIX

This appendix is divided into two sections. The first section, titled "R Scripts," includes all the code used for the phylogenetic imputation process, ecological characterization, and the creation of the input dataset for the PyRate analysis. The second section, titled "PyRate Command Lines," provides examples of the command lines used for the preliminary diversification analysis and age-dependent analysis. Please note that the code files used to generate the figures presented in both the main text and supplementary material are not listed here. However, they can be made available upon request to the author at any time.

The data utilized in this study were sourced from publicly accessible databases and primary literature. Fossil occurrence data were obtained from the Paleobiology Database (PBDB, https://paleobiodb.org/#/) and the New and Old Worlds Fossil Mammal Database (NOW, https://nowdatabase.org). Interested parties can also access this dataset by selecting "Canidae" as the taxonomic group of interest and following the data curation protocol outlined in the methods section of this study. Morphological data used in the Ecological Characterization were sourced from Slater (2015) and Faurby *et al*. (2021) and can be found in the Dryad digital repository (https://doi.org/10.5061/dryad.9qd51 and https://doi.org/10.5061/dryad.fttdz08t5, respectively). The morphological data for extant carnivores used in the training set were taken from Slater (2015), and the diet classification used is present in Supplementary Table 1.
The phylogenetic information for all carnivores used in this study was taken from Faurby *et al*. (2019) (https://www.biorxiv.org/content/10.1101/755207v1.supplementary-material).

To ensure the reproducibility of our analyses, we intend to make both the data and scripts available in a specific format for analysis on the Dryad repository (datadryad.org) once the study results are published.

R Scripts

"Creating_canidae_trees_script. R" code file

```
# Canidae Trees Script
#Load necessary libraries
require(ape)
# Read Carnivora trees from a Nexus file. Trees were taken from Faurby et al (2019)
Carnivora_trees <- read. nexus (file = "Carnivora.nex")

# Read Canidae species data from a CSV file. Data were taken from Slater (2015) and
Faurby et al (2021). It represents the compilation of species from which we have
morphological data and fossil occurrences.
canids_species <- read.csv ("Species_data.csv", header = TRUE, sep = ";") # file
with all information from canids
```

```
# Create an empty list for Canidae trees
Canidae_trees <- as. list (rep (NA, length (Carnivora_trees)))

# Check if species names in Carnivora trees match those in the Canidae species data
check <- name. check (Carnivora_trees [[1]], canids_species$lineage)

# Iterate through each tree and retain only Canidae species
for (i in 1: length (Carnivora_trees)) {
  Canidae_trees[[i]] <- keep.tip (Carnivora_trees[[i]], canids_species$lineage)
}
# Ensure non-zero edge lengths to avoid numerical issues
for (i in 1: length (Canidae_trees)) {
  Canidae_trees[[i]] $edge. length [which (Canidae_trees[[i]] $edge. length == 0)]
<- 0.00000000001
}
# Write the Canidae trees to a file
write. tree (Canidae_trees, file = "Canidae_trees. tree")
```

"Imputation_script. R" code file

```
#Script to perform the phylogenetic imputation
# Load necessary packages
require(phytools)
require(geiger)
require(dplyr)
require (Rphylopars)

# Read the Canidae tree data
Canidae_trees <- read. tree (file = "Canidae_trees. tree")

# Read the file eco_morph with information about the ecomorphological data. This
represents the compilation of morphological and ecological data taken from Slater
(2015) and Faurby et al (2021) and fossil occurrences.
df <- read.csv (file = "eco_morph.csv", header = TRUE, sep = ";")
data <- df [, -c (8,9)] #removing variables that we are not going to use in the
#imputation.

# Create a list to store ordered data
list_data <- list ()
```

```
# Loop to order species data to match the tree tips
for (i in 1: length (Canidae_trees)) {
  data_order <- data [match (Canidae_trees[[i]] $tip. label, data$species),]
  list_data[[i]] <- data_order
}

# Create lists to store imputation data and lambda reconstructions
imputation_data <- list ()
p_lambda_ancrecon <- list ()

# Loop through the trees and perform imputation
for (i in 1: length (Canidae_trees)) {
  p_lambda <- phylopars (
    trait_data = list_data[[i]],
    tree = Canidae_trees[[i]],
    phylo_correlated = TRUE,
    pheno_correlated = FALSE,
    model = "lambda"
  )
  p_lambda_ancrecon[[i]] <- p_lambda$anc_recon [1:133,] [order (rownames
(p_lambda$anc_recon [1:133,])),]
  imputation_data[[i]] <- p_lambda
}

# Create a list to store lambda reconstructions as data frames
p_lambda_dataframe <- list ()

# Convert lambda reconstructions to data frames
for (i in 1: length (Canidae_trees)) {
  p_lambda_dataframe[[i]] <- as.data. frame(p_lambda_ancrecon[[i]])
}

# Calculate row means for specified columns and create a data frame
columns_to_mean <- c ("RLGA", "RBL", "M2S", "M1BS", "p4S")
species_means_list <- lapply (p_lambda_dataframe, function(df) {
  row_means <- rowMeans (df [, columns_to_mean, drop = FALSE])
  return(row_means)
})
```

```
df_list <- as.data. frame (do. call (cbind, species_means_list))
colnames(df_list) <- columns_to_mean
row. names(df_list) <- row. names (p_lambda_dataframe [[1]])

# Add the MAT column from the original data frame
df_list <- cbind (df_list, MAT = df$MAT)

# Write the final data frame to a CSV file with the imputed values and the MAT
variable
write.csv (df_list, "Imput_values.csv")
```

"Discriminant_analysis_script. R" code file

```
# Linear Discriminant Analysis. Strongly based on the code provided by Slater
(2015)
# Load the required library MASS for LDA
require (MASS)

# Load training data from a CSV file - this file contains the morphological data
for extant carnivores taken from Slater (2015) and the diet classifications used
are present in the supplementary table 1

ed <- read.csv ("Training_set.csv", header = TRUE, sep = ";", row. names =
"species")

# Fossil data
fd <- read.csv ("Imput_values.csv", header = TRUE, sep = ";", row. names =
"species")
na.foo <- function(x) sum (! is.na(x))

# TS1 Based on Hopkins et al (2021) ecological classification ---------------------
-----------------------------------------

# First LDA (TS1) -----------------------------------------------------------------
disc_TS1 <- lda (TS1_diet ~ RLGA + RBL + M1BS + M2S + MAT + p4S, data = as.data.
frame(ed))
dis. pred_TS1 <- predict(disc_TS1)
disc_TS1
```

```
# Visualization and storage of LDA results for TS1
resultados_lda1_TS1 <- cbind(rownames(ed), ed[,"TS1_diet"], dis. pred_TS1$class)
plot (dis. pred_TS1$x, pch = 21, bg = dis. pred_TS1$class)
text (dis. pred_TS1$x, label = rownames (dis. pred_TS1$x), cex = 0.4)
coef(disc_TS1)

# Selection of extant species of interest for TS1
extant_TS1 <- cbind (dis. pred_TS1$class, dis. pred_TS1$posterior, dis. pred_TS1$x)
canids_extant_TS1 <- extant_TS1[c ("Canis_latrans", "Canis_lupus", "Cuon_alpinus",
"Urocyon_cinereoargenteus", "Vulpes_lagopus", "Vulpes_velox", "Vulpes_vulpes"),
(1:6)]

# Classification of fossil data for TS1
fd. pred_TS1 <- predict (disc_TS1, as.data. frame(fd))
fossil. classif_TS1 <- cbind (fd. pred_TS1$class, fd. pred_TS1$posterior, fd.
pred_TS1$x)
fossil. classif1_TS1 <- fossil. classif_TS1[-which (is.na (fossil.
classif_TS1[,1])),]
unclass_TS1 <- which (is.na (fossil. classif_TS1[,1]))
apply(fd[unclass_TS1,], 2, na.foo)

# Second LDA (TS1) ---------------------------------------------------------------

# Exclude the MAT variable from LDA for TS1
disc_TS1 <- lda (TS1_diet ~ RLGA + RBL + M1BS + M2S + p4S, data = as.data.
frame(ed))
disc_TS1
coef(disc_TS1)
dis. pred_TS1 <- predict(disc_TS1)
resultados_lda2_TS1 <- cbind(rownames(ed), ed[,"TS1_diet"], dis. pred_TS1$class)

# Visualization of results from the second LDA for TS1
plot (dis. pred_TS1$x, pch = 21, bg = dis. pred_TS1$class)
text (dis. pred_TS1$x, label = rownames (dis. pred_TS1$x), cex = 0.4)

# Classification of fossil data using the second LDA for TS1
fd. pred2_TS1 <- predict (disc_TS1, as.data. frame(fd))
```

```
fossil. classif.2_TS1 <- cbind (fd. pred2_TS1$class, fd. pred2_TS1$posterior, fd.
pred2_TS1$x)

fossil. classif_2_TS1 <- fossil. classif.2_TS1[which (is.na (fossil.
classif_TS1[,1])),]
unclass_TS1 <- which (is.na (fossil. classif_2_TS1[,1]))

# Confirmation that there are no missing classifications for TS1
apply(fd[unclass_TS1,], 2, na.foo)
# Results of discriminant classification for TS1
discr_result_TS1 <- rbind (na. omit (fossil. classif_TS1[, (1:6)]), fossil.
classif_2_TS1[, (1:6)])

# Obtaining diet information for TS1
diet_TS1 <- discr_result_TS1[match(rownames(fd), rownames(discr_result_TS1)),1]

# Create the complete dataset (133 species) with diet information for TS1
TS1 <- rbind (na. omit (fossil. classif_TS1[, (1:6)]), fossil. classif_2_TS1[,
(1:6)], canids_extant_TS1)
write.csv (TS1, "LDA_TS1_final.csv")

# TS2 Based on Slater (2015) ecological classification-----------------------------
----------------------------------

# First LDA (TS2) ----------------------------------------------------------------
disc_TS2 <- lda (TS2_diet ~ RLGA + RBL + M1BS + M2S + MAT + p4S, data = as.data.
frame(ed))
dis. pred_TS2 <- predict(disc_TS2)
disc_TS2

# Visualization and storage of LDA results for TS2
resultados_lda1_TS2 <- cbind(rownames(ed), ed[,"TS2_diet"], dis. pred_TS2$class)
plot (dis. pred_TS2$x, pch = 21, bg = dis. pred_TS2$class)
text (dis. pred_TS2$x, label = rownames (dis. pred_TS2$x), cex = 0.4)
coef(disc_TS2)

# Selection of extant species of interest for TS2
extant_TS2 <- cbind (dis. pred_TS2$class, dis. pred_TS2$posterior, dis. pred_TS2$x)
```

```
canids_extant_TS2 <- extant_TS2[c ("Canis_latrans", "Canis_lupus", "Cuon_alpinus",
"Urocyon_cinereoargenteus", "Vulpes_lagopus", "Vulpes_velox", "Vulpes_vulpes"),
(1:7)]

# Classification of fossil data for TS2
fd. pred_TS2 <- predict (disc_TS2, as.data. frame(fd))
fossil. classif_TS2 <- cbind (fd. pred_TS2$class, fd. pred_TS2$posterior, fd.
pred_TS2$x)
fossil. classif1_TS2 <- fossil. classif_TS2[-which (is.na (fossil.
classif_TS2[,1])),]
unclass_TS2 <- which (is.na (fossil. classif_TS2[,1]))
apply(fd[unclass_TS2,], 2, na.foo)

# Second LDA (TS2) ---------------------------------------------------------------

# Exclude the MAT variable from LDA for TS2
disc_TS2 <- lda (TS2_diet ~ RLGA + RBL + M1BS + M2S + p4S, data = as.data.
frame(ed))
disc_TS2
coef(disc_TS2)
dis. pred_TS2 <- predict(disc_TS2)
resultados_lda2_TS2 <- cbind(rownames(ed), ed[,"TS2_diet"], dis. pred_TS2$class)

# Visualization of results from the second LDA for TS2
plot (dis. pred_TS2$x, pch = 21, bg = dis. pred_TS2$class)
text (dis. pred_TS2$x, label = rownames (dis. pred_TS2$x), cex = 0.4)

# Classification of fossil data using the second LDA for TS2
fd. pred2_TS2 <- predict (disc_TS2, as.data. frame(fd))
fossil. classif.2_TS2 <- cbind (fd. pred2_TS2$class, fd. pred2_TS2$posterior, fd.
pred2_TS2$x)

fossil. classif_2_TS2 <- fossil. classif.2_TS2[which (is.na (fossil.
classif_TS2[,1])),]
unclass_TS2 <- which (is.na (fossil. classif_2_TS2[,1]))

# Confirmation that there are no missing classifications for TS2
apply(fd[unclass_TS2,], 2, na.foo)
```

```
# Final results of discriminant classification for TS2
discr_result_TS2 <- rbind (na. omit (fossil. classif_TS2[, (1:7)]),
fossil.class_2_TS2[, (1:7)])

# Obtaining diet information for TS2
diet_TS2 <- discr_result_TS2[match(rownames(fd), rownames(discr_result_TS2)),1]

# Create the complete dataset (133 species) with diet information for TS2
TS2 <- rbind (na. omit (fossil. classif_TS2[, (1:7)]), fossil. classif_2_TS2[,
(1:7)], canids_extant_TS2)
write.csv (TS2, "LDA_TS2_final.csv")

# Final table -----------------------------------------------------------

fr <- cbind (TS1[,1], TS2[,1])
colnames(fr) <- c ("TS1", "TS2")

fr <- ifelse (fr [,1:2] == 1, "hyper", ifelse (fr [,1:2] %in% c (2, 3), "non-
hyper", fr [,1:2]))
write.csv (fr, "diet_classification.csv")
```

"Input_pyrate_diet. R" code file

```
# Script to create the input files to PyRate - ecological pool of species
# Load required library
require(dplyr)
require(devtools)
source_url("https://raw.githubusercontent.com/dsilvestro/PyRate/master/pyrate_utili
ties.r") # load the function from the pyrate. utilities

# Read fossil occurrence dataset from PBDB
OF <- read.csv (file = "database_PBDB_NOW_occs.csv", header = TRUE, sep = ";")

# Read dietary classification data
data <- read.csv (file = "diet_classification.csv", header = TRUE, sep = ";")

# Filter species based on dietary classification (TS1/Hopkins)
hyper_hopkins <- data$diet_hopkins == "hyper"
spp_hyper <- data [hyper_hopkins, 1]
```

```
nohyper_hopkins <- data$diet_hopkins! = "hyper"
spp_nohyper <- data [nohyper_hopkins, 1]

# Filter occurrence data based on selected species (TS1/Hopkins)
OCC_hyper <- OF [OF$species %in% spp_hyper, c ("species", "status", "MinT",
"MaxT")]
OCC_nohyper <- OF [OF$species %in% spp_nohyper, c ("species", "status", "MinT",
"MaxT")]

# Rename columns
colnames (OCC_hyper) <- c ("Species", "Status", "MinT", "MaxT")
colnames (OCC_nohyper) <- c ("Species", "Status", "MinT", "MaxT")

# Write filtered occurrence data to files
write. table (OCC_hyper, "PBDB_Hopkins_Hyper_occs.txt", sep = "\t", row. names =
FALSE)
write. table (OCC_nohyper, "PBDB_Hopkins_noHyper_occs.txt", sep = "\t", row. names
= FALSE)

# Input files to PyRate analysis (TS1/Hopkins)
extract. ages (file = "PBDB_Hopkins_Hyper_occs.txt", replicates = 50)
extract. ages (file = "PBDB_Hopkins_noHyper_occs.txt", replicates = 50)

# Filter species based on dietary classification (TS2/Slater)
hyper_slater <- data$diet_slater == "hyper"
spp_hyper <- data [hyper_slater, 1]

nohyper_slater <- data$diet_slater! = "hyper"
spp_nohyper <- data [nohyper_slater, 1]

# Filter occurrence data based on selected species (TS2/Slater)
OCC_hyper <- OF [OF$species %in% spp_hyper, c ("species", "status", "MinT",
"MaxT")]
OCC_nohyper <- OF [OF$species %in% spp_nohyper, c ("species", "status", "MinT",
"MaxT")]

# Rename columns
colnames (OCC_hyper) <- c ("Species", "Status", "MinT", "MaxT")
```

```
colnames (OCC_nohyper) <- c ("Species", "Status", "MinT", "MaxT")

# Write filtered occurrence data to files (TS2/Slater)
write. table (OCC_hyper, "PBDB_Slater_Hyper_occs.txt", sep = "\t", row. names =
FALSE)
write. table (OCC_nohyper, "PBDB_Slater_noHyper_occs.txt", sep = "\t", row. names =
FALSE)

# Create the input files to PyRate analysis (TS2/Slater)
extract. ages (file = "PBDB_Slater_Hyper_occs.txt", replicates = 50)
extract. ages (file = "PBDB_Slater_noHyper_occs.txt", replicates = 50)
```

"Input_pyrate_families. R" code file

```
# Script to create the input files to PyRate Analysis - phylogenetic pools of
species
# Load required libraries
require(dplyr)
require(devtools)

# Load the PyRate utilities function from GitHub
source_url("https://raw.githubusercontent.com/dsilvestro/PyRate/master/pyrate_utili
ties.r")

# Read the fossil occurrence dataset from PBDB
OF <- read.csv (file = "database_PBDB_NOW_occs.csv", header = TRUE, sep = ";")

# Create a 'genera' column
OF$genera <- sub (pattern = "_. *", "", OF$species)

# Add the 'family' column as NA
OF$family <- NA

# Assign families based on genera
OF$family [OF$genera %in% c ("Cynodesmus", "Caedocyon", "Ectopocynus",
"Enhydrocyon", "Hesperocyon", "Mesocyon", "Osbornodon", "Paraenhydrocyon",
"Philotrox", "Sunkahetanka")] <- "Hesperocyoninae"
```

```
OF$family [OF$genera %in% c ("Aelurodon", "Archaeocyon", "Borophagus", "Carpocyon",
"Cormocyon", "Cynarctoides", "Cynarctus", "Desmocyon", "Epicyon","Euoplocyon",
"Metatomarctus", "Microtomarctus", "Otarocyon", "Oxetocyon", "Paracynarctus",
"Paratomarctus", "Phlaocyon", "Protepicyon", "Protomarctus", "Psalidocyon",
"Rhizocyon", "Tephrocyon", "Tomarctus")] <- "Borophaginae"

OF$family [OF$genera %in% c ("Canis", "Cerdocyon", "Chrysocyon", "Cuon", "Eucyon",
"Leptocyon", "Metalopex", "Theriodictis", "Urocyon", "Vulpes", "Xenocyon")] <-
"Caninae"

# Extract subfamily data into separate data frames
Borophaginae <- OF [which (OF$family == 'Borophaginae'), c ("species", "status",
"MinT", "MaxT")]
Hesperocyoninae <- OF [which (OF$family == 'Hesperocyoninae'), c ("species",
"status", "MinT", "MaxT")]
Caninae <- OF [which (OF$family == "Caninae"), c ("species", "status", "MinT",
"MaxT")]

# Rename columns for subfamily data
colnames (Borophaginae) <- c ("Species", "Status", "MinT", "MaxT")
colnames (Hesperocyoninae) <- c ("Species", "Status", "MinT", "MaxT")
colnames (Caninae) <- c ("Species", "Status", "MinT", "MaxT")

# Write subfamily data to separate files
write. table (Borophaginae, "PBDB_Borophaginae_occs.txt", sep="\t", row.
names=FALSE)
write. table (Hesperocyoninae, "PBDB_Hesperocyoninae_occs.txt", sep="\t", row.
names=FALSE)
write. table (Caninae, "PBDB_Caninae_occs.txt", sep="\t", row. names=FALSE)

# Extract ages from subfamily files
extract. ages (file = "PBDB_Borophaginae_occs.txt", replicates = 50)
extract. ages (file = "PBDB_Hesperocyoninae_occs.txt", replicates = 50)
extract. ages (file = "PBDB_Caninae_occs.txt", replicates = 50)

# Extract data for the broader family Canidae
canidae <- OF [, c ("species", "status", "MinT", "MaxT")]

# Rename columns for the Canidae data
```

```
colnames(canidae) <- c ("Species", "Status", "MinT", "MaxT")

# Write Canidae data to a file
write. table (canidae, "PBDB_Canidae_occs.txt", sep="\t", row. names=FALSE)

# Extract ages from the Canidae data
extract. ages (file = "PBDB_Canidae_occs.txt", replicates = 50)
```

PyRate command lines

In this section, we list the command lines employed within PyRate for conducting both the preliminary diversification analysis and the age-dependent analysis. Within these command lines, the Python parameter "-j" pertains to each individual replicated dataset. In the provided examples, we use "-j 1" to denote the first temporal replicated dataset out of a total of 50 such replicated datasets. The file “TPP_shifts.txt” corresponds to a ".txt" file used to define the different time windows of preservation used in the analysis. The file has the following content: 20.43, 4.9 for all analyses except in Hesperocyoninae which used the following values: 30.8, 20.3.

Preliminary diversification analysis

Hesperocyoninae

```
python3 PyRate.py PBDB_Hesperocyoninae_occs_PyRate.py -A 4 -mG -qShift
TPP_shifts.txt -n 60000000 -s 10000 -p 10000 -j 1
```

Borophaginae

```
python3 PyRate.py PBDB_Borophaginae_occs_PyRate.py -A 4 -mG -qShift TPP_shifts.txt
-n 60000000 -s 10000 -p 10000 -j 1
```

Caninae

```
python3 PyRate.py PBDB_Caninae_occs_PyRate.py -A 4 -mG -qShift TPP_shifts.txt -n
60000000 -s 10000 -p 10000 -j 1
```

Canidae

```
python3 PyRate.py PBDB_Canidae_occs_PyRate.py -A 4 -mG -qShift TPP_shifts.txt -n 60000000 -s 10000 -p 10000 -j 1
```

Hypercarnivores – TS1/Hopkins

```
python3 PyRate.py PBDB_Hopkins_Hyper_occs_PyRate.py -A 4 -mG -qShift TPP_shifts.txt -n 60000000 -s 10000 -p 10000 -j 1
```

Non-Hypercarnivores TS1/Hopkins

```
python3 PyRate.py PBDB_Hopkins_noHyper_occs_PyRate.py -A 4 -mG -n 60000000 -s 10000 -p 10000 -j 1
```

Hypercarnivores – TS2/Slater

```
python3 PyRate.py PBDB_Slater_Hyper_occs_PyRate.py -A 4 -mG -qShift TPP_shifts.txt -n 60000000 -s 10000 -p 10000 -j 1
```

Non-Hypercarnivores – TS2/Slater

```
python3 PyRate.py PBDB_Slater_noHyper_occs_PyRate.py -A 4 -mG -n 60000000 -s 10000 -p 10000 -j 1
```

Age-dependent analysis

Hesperocyoninae 01

```
python3 PyRate.py PBDB_Hesperocyoninae_occs_PyRate.py -A 4 -qShift TPP_shifts.txt -n 2000000 -s 10000 -p 10000 -ADE 1 -j 1 -filter inf 17.6
```

Borophaginae 01

```
python3 PyRate.py PBDB_Borophaginae_occs_PyRate.py -A 4 -qShift TPP_shifts.txt -n 2000000 -s 10000 -p 10000 -ADE 1 -j 1 -filter inf 16.75
```

Borophaginae 02

```
python3 PyRate.py PBDB_Borophaginae_occs_PyRate.py -A 4 -mHPP -n 2000000 -s 10000 -p 10000 -ADE 1 -j 1 -filter 16.75 7
```

Borophaginae 03

```
python3 PyRate.py PBDB_Borophaginae_occs_PyRate.py -A 4 -mHPP -n 2000000 -s 10000 -p 10000 -ADE 1 -j 1 -filter inf 7
```

Caninae 01

```
python3 PyRate.py PBDB_Caninae_occs_PyRate.py -A 4 -qShift TPP_shifts.txt -n 2000000 -s 10000 -p 10000 -ADE 1 -j 1 -filter inf 3.5
```

Canidae 01

```
python3 PyRate.py PBDB_Canidae_occs_PyRate.py -A 4 -mHPP -n 2000000 -s 10000 -p 10000 -ADE 1 -j 1 -filter inf 19
```

Canidae 02

```
python3 PyRate.py PBDB_Canidae_occs_PyRate.py -A 4 -mHPP -n 2000000 -s 10000 -p 10000 -ADE 1 -j 1 -filter 17 3
```

Canidae 03

```
python3 PyRate.py PBDB_Canidae_occs_PyRate.py -A 4 -qShift TPP_shifts_ADE.txt -n 2000000 -s 10000 -p 10000 -ADE 1 -j 1 -filter inf 3
```

TS1 Hypercarnivores 01

```
python3 PyRate.py PBDB_Hopkins_Hyper_occs_PyRate.py -A 4 -qShift TPP_shifts.txt -n 2000000 -s 10000 -p 10000 -ADE 1 -j 1 -filter inf 6.85
```

TS1 Non-Hypercarnivores 01

```
python3 /PyRate.py PBDB_Hopkins_noHyper_occs_PyRate.py -A 4 -qShift TPP_shifts.txt -n 2000000 -s 10000 -p 10000 -ADE 1 -j 1 -filter inf 18
```

TS1 Non-Hypercarnivores 02

```
python3 PyRate.py PBDB_Hopkins_noHyper_occs_PyRate.py -A 4 -mHPP -n 2000000 -s 10000 -p 10000 -ADE 1 -j 1 -filter 14.5 0
```

TS2 Hypercarnivores 01

```
python3 PyRate.py PBDB_Slater_Hyper_occs_PyRate.py -A 4 -qShift TPP_shifts.txt -n 2000000 -s 10000 -p 10000 -ADE 1 -j 1 -filter inf 6.85
```

TS2 Non-Hypercarnivores 01

```
python3 PyRate.py PBDB_Slater_noHyper_occs_PyRate.py -A 4 -qShift TPP_shifts.txt -n
2000000 -s 10000 -p 10000 -ADE 1 -j 1 -filter inf 18
```

TS2 Non-Hypercarnivores 02

```
python3 PyRate.py PBDB_Slater_noHyper_occs_PyRate.py -A 4 -mHPP -n 2000000 -s 10000
-p 10000 -ADE 1 -j 1 -filter 14.5 0
```